PB92-109255

Fundamental Factors That Affect Dust Generation

North Carolina Univ. at Chapel Hill. Dept. of Environmental Sciences and Engineering

Prepared for:

National Inst. for Occupational Safety and Health, Cincinnati, OH

31 May 91

50272-101

REPORT DOCUMENTATION PAGE	1. REPORT NO.	2.	3. PB92-109255

4. Title and Subtitle: Fundamental Factors that Affect Dust Generation

5. Report Date: 1991/05/31

6.

7. Author(s): Leith, D.

8. Performing Organization Rept. No.

9. Performing Organization Name and Address: Department of Environmental Sciences and Engineering, University of North Carolina, Chapel Hill, North Carolina

10. Project/Task/Work Unit No.

11. Contract (C) or Grant(G) No.
(C)
(G) R01-OH-02437

12. Sponsoring Organization Name and Address

13. Type of Report & Period Covered

14.

15. Supplementary Notes

16. Abstract (Limit: 200 words) Factors that affect the amount and size distribution of dust generated by falling granular material in still air were examined using an apparatus with separate dust generating and measuring sections. Four granular materials were tested and a simple model was developed to describe the dust generation rate of these materials as a function of particle size, drop height, material flow, and moisture content. Moisture content strongly influenced the interparticle binding forces and the amount of dust generated. Drop height and material flow influenced the material separation forces and also showed significant influence on the amount of dust generated. In a second study, four factors that affect dust generation (test material, size distribution of the test material, moisture content of the test material, and the apparatus used for the tests) were investigated. Dust generated from silicon-carbide (409212) and aluminum-oxide (1344281) were measured using magnetic resonance imaging and Heubach dustiness testers. The size distribution of the test material slightly influenced the amount but strongly influenced the size distribution of the dust generated. Increased moisture content decreased the amount of dust generated but had little influence on dust size distribution.

17. Document Analysis a. Descriptors

b. Identifiers/Open-Ended Terms: NIOSH-Publication, NIOSH-Grant, Grant-Number-R01-OH-02437, End-Date-11-30-1990, Control-technology, Airborne-dusts, Physical-properties, Airborne-particles, Aerosols, Dust-particles

c. COSATI Field/Group

18. Availability Statement	19. Security Class (This Report)	21. No. of Pages 60
	22. Security Class (This Page)	22. Price

(See ANSI-Z39.18) *See Instructions on Reverse*

OPTIONAL FORM 272(4-77)
(Formerly NTIS 35)
Department of Commerce

Fundamental Factors that Affect Dust Generation

Final Report for PHS-CDC Grant 5 RO1 OH02437

PI: David Leith
Department of Environmental Sciences and Engineering
Rosenau Hall, CB 7400
University of North Carolina
Chapel Hill, NC 27599-7400

31 May 1991

CONTENTS

LIST OF ABBREVIATIONS

C	dust concentration, mg/m^3
d	particle diameter
d_{min}	minimum particle diameter of test material
d_{50}	mass median diameter of the parent material
D	material bulk density, g/cm^3
D_i	average diameter of the particles collected on the impactor
F	material flow, kg/s
$Frac_i$	mass fraction of test material with size "i".
G_i	fraction of dust particles generated with diameter "i"
H	drop height, m
k_i	empirical parameter that depends on particle size
L	MRI dustiness test index
M	is the mass of the dropped material (kg)
M_D	total mass of dust generated
$(M_D)_i$	mass of dust generated with size "i"
M_g	mass median diameter of the parent material
M_M	total mass of test material
$(M_M)_i$	mass of test material with size "i"
MRI	Midwest Research Institute
$Q_3(d)$	cumulative size distribution of the generated dust
S	"silt content" of the dropped material, %
SEM	Scanning Electron Microscope
S_g	geometric standard deviation of the parent material
T	material type
V	is the crosswind velocity, km/hr
W	Moisture content, mass fraction

LIST OF FIGURES

LIST OF TABLES

Experimental Examination of Factors that Affect Dust Generation

MARC A.E. PLINKE, DAVID LEITH, DAVID B. HOLSTEIN, AND MARYANNE G. BOUNDY

Department of Environmental Sciences and Engineering, University of North Carolina at Chapel Hill, Chapel Hill, NC 27599

A method is presented to examine factors that affect the amount and size distribution of dust generated by falling granular material in still air. This work was conducted using an apparatus with separate dust generating and dust measuring sections. The dust generated by a falling material was carried into an elutriation column equipped with a slotted Sierra high volume impactor at the top. This apparatus can measure dust generation rates for particles between 0.4 and 25 um in aerodynamic diameter as well as the amount of air entrained by the falling material. Four granular materials were tested, and a simple model was developed to describe the dust generation rate of these materials as a function of particle size, drop height, material flow, and moisture content. Moisture content strongly influenced the interparticle binding forces and the amount of dust generated. Drop height and material flow influenced the material separation forces and also showed significant influence on the amount of dust generated.

BACKGROUND

Powders and granulated solids are used throughout industry. The handling of these materials at locations such as transfer points or bagging and dumping operations generates dust that may affect worker health, create a safety problem, or cause a nuisance. To evaluate the extent of these hazards, the dust concentration in the breathing zone of the worker must be determined. This concentration depends both on the dust generation rate of the material and its dispersion. The focus of this research was to investigate factors that affect dust generation

rate as a function of particle size.

The hypothesis examined here was that dust generation depends on the ratio of forces that separate granular material to forces that bind granular material together,

$$\textit{Dust Generation Rate} = f(\textit{Separation forces/Binding forces}) \quad (1)$$

Both mass generation rate and size distribution of the generated dust are important; generation rate determines mass concentration whereas size distribution affects dispersion throughout the workplace and determines where inhaled particles collect in the respiratory tract. Previous methods to assess dustiness have not always adequately addressed the interdependence of these two factors.

Although several methods to evaluate dust generation have been developed [1,2], no comprehensive or fundamental investigation of the separation forces, the binding forces, or their interaction has been reported. Consequently, little quantitative knowledge exists concerning fundamental factors that affect dust generation.

The British Occupational Hygiene Society [3] established a working group in 1981 to develop a procedure to measure "dustiness", to establish a dustiness index scale, and to correlate the measured dustiness with actual worker exposure. Although this group has evaluated eighteen measurement devices, to date neither a correlation study nor a dustiness index scale has been established. However, the working group did categorize these devices by the manner the separation forces were created - through gravitational, mechanical or gas dispersion techniques. In addition, they found drop height and sample mass are important variables that influence dust generation.

Higman *et al.* [4] ranked the dustiness of nine materials using three types of dustiness devices that simulate different handling operations. They found that the dustiness rankings

produced by each device agreed well with each other, thus confirming that the dustiness rankings were dependent on the materials themselves rather than on the devices used to assess dustiness. This group also investigated the influence of some binding forces on dust generation. Contradicting their earlier work [5], they found that increasing the proportion of coarse particles in some bulk materials may actually *increase* dustiness. This unintuitive result was confirmed by Upton et al. [6] and was attributed to the "decrease in the cohesion of the material as the proportion of coarse particles increases" and by the agitation of the fine particles caused by the increased number of collisions with large particles.

Investigators at the Warren Springs Laboratory in the UK [5] examined the effect of moisture content on dust generation. Using a fluidized bed device they found that the binding forces strongly depended on the size distribution and moisture content of the test material. A decrease in dustiness occurred if the particle mass or size was increased or if moisture was added.

Cowherd and co-workers[2,7] at the Midwest Research Institute (MRI) developed a bench-top dust chamber to measure the dustiness of a fixed volume of granulated materials dropped from a fixed height. After testing fourteen materials they developed a four-parameter model for dustiness potential that accounted for 71% of the variation observed in their material dustiness tests. The model correlates the fractional mass loss, L (mg of dust per kilogram of material dropped), as

$$L = 16.6(W)^{-0.75}(S_g)^{3.9}(D)^{-1.2}(M_g)^{-0.45}, \qquad (2)$$

where

W is the moisture content (%),

S_g is the geometric standard deviation of the size distribution for the dropped material,

D is material bulk density (g/cc), and

M_g is the mass median diameter (um) of the size distribution for the dropped material.

Heitbrink et al. at NIOSH conducted the only field studies in the literature that attempt to correlate dustiness indices from the MRI and the Heubach rotating drum tester[8] with personal dust exposures of workers [9-11]. In some field evaluations they found no correlation; in others, they found significant correlation between personal exposure and drop height, geometric mean particle size, and fines content. However in most of the studies they found that plant conditions, process variables, and the work habits and body stature of the workers were more important variables than dustiness. From these data Heitbrink and O'Brien [12] developed a regression model relating the worker dust exposure (mg/m^3), C, to the MRI dustiness test index, L,

$$C = 0.82\ exp(0.0086\ L). \qquad (3)$$

The R^2 for this model was 0.5 and the confidence level is less than 0.0001. Using this model the authors proposed an exposure prediction logic relating the MRI index to the maximum predicted exposure of the worker.

Other studies evaluating dust problems in industry have been undertaken with a specific goal in mind or have examined the problems of only one material or operation. For example, the dispersion of alumina dust generated during handling operations results in a loss of 10,000 MT/year of alumina per reduction plant and has forced this industry to examine dustiness. Using a Perra pulvimeter, whereby a known volume of alumina is dropped from a funnel onto an inverted cone, Hseih [13] showed the importance of moisture content and amounts of added calcined dust from an electrostatic precipitator in controlling dispersion. Authier-Martin [14] found that dust particle shape may be the critical parameter. Scanning electron microscope

pictures (SEMs) of the air-borne particles showed that "clean" alumina (as ranked by the Perra pulvimeter) generated dusts of coarse particles with a cohesive mosaic type structure, whereas the dustier alumina consisted of smaller, single crystals.

Outdoor studies of air pollution in which processed steel slag and crushed limestone were dropped from the bucket of a front-end loader offer some quantitative methods by which dust generation rates can be estimated. These studies [15,16] correlated the generation rate for particles of aerodynamic diameter "i", G_i as

$$G_i = k_i \, (S \, V \, H \, M^{2/3})/(W^2) \quad . \tag{4}$$

Here,

- k_i is an empirical parameter that depends on particle size,
- S is the "silt content" of the dropped material (%),
- V is the crosswind velocity (km/hr),
- H is the drop height (m),
- M is the mass of the dropped material (kg), and
- W is the water content (%).

These studies have examined several factors that affect dust generation. They suggest that binding forces are influenced by moisture content, size distribution and shape of the material, and in one case by the addition of electrostatic precipitator dusts. The separation forces are influenced by crosswinds, drop height, and, in one case, sample mass. Additional factors influencing the dust exposure are process variables such as work habits and worker body structure.

No fundamental study of all these variables has been conducted using one test method or apparatus. Furthermore, the effect of material flow and the amount of air entrained with a

falling stream of material has not been investigated. Thus, the aims of this study were to build a device and to develop a procedure to investigate the effects of material type, moisture content, drop height, material flow, and entrained air.

EXPERIMENTS

Apparatus

Figure 1 shows the apparatus built to evaluate factors that affect dust generation in terms of particle size. This apparatus has two sections: the dust generation section on the left and the dust measurement section on the right. Separation of the generation and measurement sections allows independent examination of dust generation and dust transport mechanisms.

To conduct a test, a granular material falls from a known height at a measured rate and passes through a hole centered on the lid of the receiving hopper. Within this hopper the falling material hits a natural pile of the same material built under the same conditions as the experiment. Air is entrained with material as it enters the hopper. From the receiving hopper the dusty air is drawn through a wide slot into the measurement area by fan "B". When all the material has fallen into the hopper, fan "B" is turned off. In the dust measurement area fan "A" circulates air through an elutriation column and an air return channel. The elutriation column prevents particles larger than 25 um in aerodynamic diameter from reaching the column top. Particles smaller than 25 um in aerodynamic diameter are carried up the elutriation column to a slotted Sierra (Andersen) model 236 impactor [17] that separates particles into the size categories shown in Table 1.

Before every experiment the aluminum substrates on each collecting stage of the impactor were coated with a silicone spray to prevent particle bounce. Then the substrates were allowed to dry for at least 24 hours before being weighed. After each experiment, the impactor substrates were removed and reweighed. Blanks of the coated substrates and the backup filter

were used with each experiment.

Two different variables can be used to present the results. The size specific dust generation rate, G_i, which is defined as the fraction of dust particles generated with aerodynamic diameter "i".

$$G_i = (M_D)_i/(M_M)_i = (M_D)_i/(M_M{*}Frac_i) \quad , \tag{5}$$

where:

$(M_D)_i$ mass of dust generated with size "i"

$(M_M)_i$ mass of test material with size "i"

M_M total mass of test material, and

$Frac_i$ mass fraction of test material with size "i".

For example, a G_4 of 0.01 indicates that 1% of the 4 μm particles in the test material is generated and collected as a dust particle.

The total dust generation rate G is the ratio of the *total* mass of dust collected with the impactor to the *total* mass of material tested. G describes the dustiness of a material without consideration of the size distribution of the original material or the size distribution of the dust generated.

$$G = M_D/M_M = \Sigma(M_D)_i / \Sigma(M_M)_i = \Sigma(M_D)_i / M_M \quad , \tag{6}$$

where:

M_D total mass of dust generated.

For example, a G of 0.01 indicates that 1% of the total mass of material becomes dust.

The amount of air entrained with the falling material V (m^3/h) was measured by adjusting the flow through fan "B". Air flow was measured with a thermal anemometer placed upstream

of fan "B". The anemometer reading was related to volumetric flow through the pipe by calibration using a spirometer. The "correct" airflow was drawn through fan "B" when there was no pressure difference between the receiving hopper and environment as detected by a smoke tube placed just outside the vent of the receiving hopper.

Procedure

Four inexpensive, readily available dusty materials were selected. Sand and limestone were chosen as examples of inorganic, crystalline substances that are nonporous and nonreactive with water. Cement and flour were selected as examples of inorganic and organic substances that are internally porous and reactive with water. The size distributions of these materials were measured before conducting the experiments using sieves[18] in mesh sizes from 2 mm to 38 um for coarse particles and an Andreasen sedimentation pipette[19] for particles finer than 38 um. Experiments were conducted with these four materials to determine the effects of the moisture content of the parent material, drop height, and mass flow rate on the amount and size distribution of dust generated.

Moisture content, *W*

The moisture content of the materials was determined by the loss of weight per unit mass of each substance after drying. Sand, cement, and limestone were dried for several days at 110°C; flour was dried at 60°C. Moisture content was raised for sand and limestone by adding a measured amount of water to a known mass of material. To reduce agglomeration of the cement and flour, moisture was added by exposing the material to steam in an autoclave.

Drop Height, *H*

Each substance was dropped from the material hopper through a funnel with an interchangeable tube into the receiving hopper. The measured drop height was the distance from the lower end of the tube to the top of the pile in the receiving hopper. This drop height

could be adjusted from 0 to 200 cm to represent part of the drop height range found in industry.

Material Flow, *F*

Total mass flow was determined by measuring the time necessary to drop a known mass of material. Flow varied from 0.1 to 10 kg/s by changing the diameter of the tube through which the material flowed. The total mass dropped varied between two and ten kilograms per test.

Measurements

The experiments had a central composite design [20] as shown in Table 2. For each test material, five replicate drops were conducted with the base values of all three variables. To determine the influence of each of the three variables in generating dust, each variable was set at its high or low value listed in Table 2 in turn, while the two other variables were set at their base values. Each of these six tests was run twice for a total of $5+12 = 17$ tests for each material. If results from the two replicates did not agree within a range of 10 %, the experiment was repeated up to five times. All results were used for data analysis.

Table 2 shows that the variable ranges were different for each material. Mass flow was regulated by the diameter of the tube below the hopper. Three tubes, 24, 37, and 49 mm in diameter, were used. The resulting flows were dependent on the material and bulk density as well as on the flowability of the examined material. Drop height changes were held constant for limestone, cement, and flour. Sand was the least dusty material and only generated enough dust for measurement at the elevated height. The moisture content of the material as received was its base value. The high values were limited by the minimum amount of dust on each impactor stage that could be weighed accurately. Low values were determined by the degree to which the materials could be dried and then handled without reabsorbing moisture from the environment. When cement was moistened, agglomerates were created that changed the size

distribution of the original material. Therefore, experiments with humidified cement were not conducted.

RESULTS

Dust generation data for all experiments with one standard deviation confidence limit are shown in Figures 2-4. Figure 2 shows the total dust generation rate, G, vs. drop height, H, for the four test materials. Although the dust generation rate increased for all materials with increasing drop height, the rate of increase differed somewhat with material.

In Figure 3 the total dust generation rate, G, is plotted vs. material flow, F, for the four test materials. Generation rate decreased with increasing material flow for sand, cement and flour, but increased for limestone.

In Figure 4 the total dust generation rate, G, is plotted vs. moisture content, W, for the four test materials. A strong dependence of generation rate on moisture content can be seen for sand and limestone; little change is evident for cement and flour.

Figure 5 shows the effects of increasing drop height on the flow of entrained air normalized to the material mass flow for three materials. The data for flour were omitted because they were below the limits of detection for the thermal anemometer.

The effect of increased material mass flow on the flow of entrained air normalized to the material mass flow is shown in Figure 6. Although the entrained air increased with increasing material flow, the volume of entrained air normalized to the material mass flow showed an overall decrease.

To determine the interactions between the dust generation rate as a function of particle size, G_i, and the three independent variables, drop height, mass flow, and moisture content, an analysis of variance for all experimental data was conducted to calculate the coefficients for the

following model:

$$G_i = const(H)^A(F)^B(W)^C(Frac_i)^E(D_i ln(Di/25))^G , \quad (7)$$

where

H is the drop height (m),

F is the material flow (kg/s),

W is the moisture content (%),

$Frac_i$ is the fraction of particles of size i in the parent material

D_i is the average diameter of the particles collected on the impactor stages

A,B,C,E,G are the calculated coefficients.

$(D_i ln(Di/25))^G$ was chosen as a function with a maximum and zero values at $D_i = 0$ and $D_i =$ 25 um. Particies with aerodynamic diameters greater than $D_i = 25$ um cannot be transported up the elutriation column to the impactor.

The resultant equations are

$$G_{i,SAND} = 0.57(H)^{1.06}(F)^{-0.69}(W)^{-0.76}(FRAC_i)^{-0.66}(D_i \ln(Di/25))^{0.87}, \quad R^2 = 0.83 \tag{8}$$

$$G_{i,LIME} = 0.56(H)^{1.51}(F)^{+0.37}(W)^{-1.60}(FRAC_i)^{-0.74}(D_i \ln(Di/25))^{1.00}, \quad R^2 = 0.92 \tag{9}$$

$$G_{i,CEMENT} = 3.42(H)^{1.02}(F)^{-0.07}(W)^{-0.32}(FRAC_i)^{-0.83}(D_i \ln(Di/25))^{1.32}, \quad R^2 = 0.93 \tag{10}$$

$$G_{i,FLOUR} = 134(H)^{1.13}(F)^{-0.36}(W)^{-2.66}(FRAC_i)^{-0.49}(D_i \ln(Di/25))^{1.47}, \quad R^2 = 0.72 \tag{11}$$

Figure 7 presents a plot of the measured dust generation rate vs. the predicted dust generation rate calculated with Eqs.(8-11).

At low material flows the falling particles were first stopped abruptly on the top of the receiving pile and then slid down the side of the pile. This phenomenon occurred for all materials. At higher flows different behavior was observed for each material. For sand, most of the falling stream penetrated the pile and displaced the material radially. For limestone, the pile was compressed by the falling stream and formed a crater 7 to 15 cm in diameter in the impact area. The crater diameter increased with material flow and drop height. Falling limestone hit the middle of the crater and bounced back in all directions. Cement behaved between the extremes of sand and limestone. The penetration of the falling stream into the receiving pile was not as deep as for sand because cement was compressed only slightly by the falling stream. No bouncing occurred and most of the falling material slid down the surface of the pile. Whereas sand, limestone, and cement built piles with flat tops, flour built a pile with a peak, which allowed the oncoming material to slide down the side of the pile without penetrating it.

DISCUSSION

The results of these experiments are consistent with the analysis of Hemeon [21], who suggested that dust is generated and dispersed by two mechanisms. First, the impact of the material as it hit the pile created separation forces that caused the material to generate dust. Second, the air entrained with the falling material must change its flow direction in the impaction area, because it cannot enter the solid pile. Therefore, a radial draft is generated which transports dust particles away from the impaction area.

Dust generation rate of different materials

A comparison of the dust generation rates for the different materials in Figures 2-4, and comparison of the leading coefficients in Eqs.(8-11) show that generation rate substantially differs among the four test materials. Since the dust generation rates for these materials were not examined under the exact same conditions for mass flow, drop height, moisture content, and size distribution, no conclusive, general statement of the dust generation behavior of different materials can be given. Nevertheless, the results strongly suggest that variations from material to material do affect dust generation substantially. This can be seen most clearly in the significantly different values of the first coefficients in Eqs.(8-11). Causes for this behavior may include variations in particle shape or surface properties from one material to the next.

Drop height

For all materials dust generation increased with increasing drop height as shown in Figure 2. Increasing drop height caused a proportional increase in the potential energy of the material before the fall and an increase of the kinetic energy of the material as it hit the receiving pile. The separation forces on the particles caused by the impact of the material on the pile should increase so that an increase in dust generation with height was expected. In addition, Figure 5

shows that increasing drop height caused an increase in flow of entrained air, which also increases the amount of dust generated. The slopes for sand, cement, and flour are nearly identical both in Figure 2 and Figure 5 which indicates a similar response to increases in energy input.

At higher drop heights, limestone produced more dust than expected from trends for other materials. Particle bouncing in the crater at a drop height of 100 cm generated high impact and separation forces, so that additional dust was generated.

Material Flow

The flow of entrained air per mass flow of dropped material decreased with increasing flow because the material in the center of the falling stream is less exposed to the surrounding air than the outside material. With higher flows, more material is present in the center of the falling stream.

For every material except limestone, dust generation rate decreased with increasing flow. For sand and cement the decrease in dust generation may be related to the relative decrease of entrained air. In addition, for these materials at higher flows the falling stream of material penetrated the receiving pile. The impact forces of the particles in this case are small, because the falling particle velocity decreased slowly in the middle of the pile. Because smaller impact forces generate smaller separating forces, less dust may be generated with higher flows for materials that penetrate the pile, such as sand and cement.

For flour the impact forces may not change, because the character of the receiving pile did not change with flow. A decrease in the dust generation rate for flour shown in Figure 3 is consistent with the decrease in entrained air shown for sand, limestone and cement in Figure 6.

The increase in dust generation rate for limestone with increasing mass flow is caused by an increase of the separation forces. Increasing the material flow above the base value created

the crater from which particles bounced as noted above. The impact forces caused by bounce were higher than the impact forces for particles of other materials which slowed gradually as they entered the pile. High impact forces caused high separation forces. Although higher flows for limestone caused a decrease in entrained air as was found for all materials, the resultant decrease in generation rate due to decreased entrained air was overcome in this case by the increase in separation forces due to particle bounce at higher flows.

Moisture Content

Increasing the moisture content of the parent material decreases dust generation as shown in Figure 4. The gradient of this decrease differs substantially from material to material. For the crystalline, non-reactive materials, limestone and sand, a small amount of water increased the surface liquid film on the particles, increasing the capillary interparticle binding forces.

The influence of moisture content on dust generation for cement and flour is smaller than for the crystalline, non-reactive materials because for cement and flour the added water did not directly influence the surface liquid film and the interparticle capillary forces. Instead, water was absorbed and reacted with the material.

The plot of predicted and actual data shows that the dust generation rate varies by more than five orders of magnitude. The reproducibility of the experimental procedure is satisfactory, since most data are within the $\pm$ 100 percent range. In addition, the chosen model (Eq.7) has the ability to describe the effects of the investigated variables on the dust generation rate, because the data points are distributed randomly above and below the perfect agreement line.

CONCLUSIONS

A device and procedure were developed to investigate factors that affect dust generation. The overall dust generation rate G, and the rate dependent on particle size G_i were the primary

variables investigated. Other variables were identified as affecting either the binding forces that hold the materials together or the separating forces that separate and disperse the materials. Their influence on dust generation was examined experimentally. Dust generation increased with the increase in separation forces caused by a higher energy input such as an increase in drop height. Dust generation decreased when the interparticle binding forces were increased by the addition of water to the parent material.

Statistical models for G_i were developed. The R^2 values of the four equations were in the range of 0.72 to 0.93. These data and the plot of predicted and actual data strongly suggest that important variables influencing dustiness have been found. The first coefficients of Eqs.(8-11) show that dust generation rate substantially differs among the four tested materials.

Additional work is necessary to develop a better understanding of the influence of binding and separation forces on dust generation. Special attention needs to focus on the influence of particle size and surface properties on G_i. A direct measurement of the falling velocity is planned to investigate more closely the effect of impact forces on dust generation.

ACKNOWLEDGEMENT

This project was supported by grant 1R01 OH02437-01 from the National Institute for Occupational Safety and Health of the Centers for Disease Control. The authors wish to thank Friedrich Loeffler, Karlsruhe, Germany for his support and advice on this project.

REFERENCES

1. **British Occupational Hygiene Society Technical Guide No. 4:** *Dustiness Estimation Methods for Dry Materials: Part 1, Their Uses and Standardization and Part 2, Towards a Standard Method.* Science Reviews Ltd., Northwood, Middx, England, in association with H and H Scientific Consultants Ltd., Leeds, England, 1985.

2. **Cowherd Jr., C., M.A.Grelinger, P.J.Englehart, R.F.Kent, and K.F.Wong:** An apparatus and methodology for predicting the dustiness of materials. *Am. Ind. Hyg. Assoc. J.* 50(3):123-130 (1989).

1. **British Occupational Hygiene Society Technology Committee Working Party on Dustiness Estimation:** Progress in dustiness estimation. *Ann. Occup. Hyg.* 32(4):535-544 (1988).

4. **Higman, R.W., C.Schofield, and M.Taylor:** "Bulk material dustiness, an important material property - its measurement and control." 4th International Environment and Safety Conference, Barbican Center, London, Mar. 27-29, 1984.

5. **Schofield, C.:** Dust generation and control in materials handling. *Bulk Solids Handling* 1(3):419-427 (1981).

6. **Upton, S.L., D.J.Hall, and G.W.Marsland:** "Some Experiments on Material Dustiness." Aerosol Society Annual Conference, University of Surrey, Guildford, Surrey, UK, April 9-11, 1990.

7. **Cowherd Jr., C., M.A.Grelinger, and K.F.Wong:** Dust inhalation exposures from the handling of small volumes of powders. *Am. Ind. Hyg. Assoc. J.* 50(3):131-138 (1989).

8. **Heubach Inc.:** *Heubach Dust Measuring Appliance.* Newark, N.J.: Heubach Inc. [Undated advertising circular]

9. **National Institute for Occupational Safety and Health:** *Control Technology for Falling Solids at Rohm and Haas Louisville, Kentucky* by W.A.Heitbrink and W.F.Todd (NIOSH Report No. ECTB 154-10). Cincinatti, Ohio, February 1987.

10. **National Institute for Occupational Safety and Health:** *Evaluation of Dustiness Test Methods and Recommendations for Improved Dust Control at Heubach Inc. Newark, New Jersey* by T.C.Cooper, W.A.Heitbrink and D.M.O'Brien (NIOSH Report No. ECTB 154-11a). Cincinatti, Ohio, February 1989.

11. **Heitbrink, W.A., W.F.Todd, T.C.Cooper, D.M.O'Brien:** The Application of Dustiness Tests to the Prediction of Worker Dust Exposure. *Am. Ind. Hyg. Assoc. J.* 51(4):217-223 (1990).

12. **National Institute for Occupational Safety and Health:** *Exposure estimation procedure for powder handling operations based on dustiness testing* by W.A.Heitbrink and D.M.O'Brien. Engineering Control Technology Branch, Division of Physical Sciences and Engineering, Cincinatti Ohio, 1989.

13. **Hsieh, H.P.:** "Measurement of flowability and dustiness of alumina." Light Metals. 1987: Proceedings of Sessions, American Institute of Mining, Metallurgical, and Petroleum Engineers (AIME) Annual Meeting, Metallurgical Soc. of AIME, Warrendale, PA. p.139-149, 1987.

14. **Authier-Martin, M.:** "Alumina handling dustiness." Light Metals, 1989: Proceedings of Sessions, AIME Annual Meeting, Metallurgical Soc. of AIME, Warrendale, PA. p.103-11, 1989.

15. **R. Bohn, T. Cuscino Jr. and C. Cowherd Jr.:** *Fugitive emissions from integrated iron and steel plants*. EPA Report EPA-600/2-78-050), Office of Research and Development, Washington DC, 20460, March 1978.

16. **US Environmental Protection Agency:** *Compilation of Emission Factors*. 3rd ed., Supplement No. 14, NTIS, Office of Air Quality Planning and Standards, Springfield, VA. p.11.23-3, 1983

17. **Willeke, K.:** Performance of the Slotted Impactor. *Am. Ind. Hyg. Assoc. J.* 36:683-691 (1975).

18. **Perry, Robert H.,ed., Don Green, ed.:** *Perry's Chemical Engineers' Handbook*. 6th ed. New York: Mc Graw Hill, 1984. pp. 21-18 - 21-19.

19. **Chen, Y.M., S.W. Doo:** An Experimental Investigation of Particle Size Analysis by a Modified Andreasen Pipet. *Powder Technology*, 48:23-29 (1986).

20. **Cochran, W.G. and G.M. Cox:** *Experimental Designs*. New York: Wiley, 1957.

21. **Hemeon, W.A.:** *Plant and Process Ventilation*, 2nd ed. New York: Industrial Press Inc., 1963, pp. 46-56

TABLE I

Cut size specifications for Sierra Model 236 high-volume cascade impactor operated at a flow of 20 cfm.

Stage	1	2	3	4	5	6	Filter
Aerodynamic Size Range, um	>25-10.2	10.2-4.2	4.2-2.1	2.1-1.4	1.4-0.73	0.73-0.41	0.41-0.00

Table II

Experimental Values of the Independent Variables

Material	Sand	Limestone	Cement	Flour
Variable	**Base/Low/Hi**	**Base/Low/Hi**	**Base/Low/Hi**	**Base/Low/Hi**
Material flow, F (kg/s)	0.5 /0.1/1.3	0.2 /.06/0.6	0.9 /0.1/2.5	.04 /.02/0.5
Drop height, H (cm)	100/50 /150	50 /25 /100	50 /25 /100	50 /25/100
Moisture content, W (%)	0.4 /0.1/0.8	0.4 /0.1/0.8	0.9 /0.1/N.A.	14 /12 /15

CAPTIONS FOR FIGURES

FIGURE 1--Schematic diagram of test apparatus.

FIGURE 2--Total dust generation rate with one standard deviation confidence limit vs. drop height.

FIGURE 3--Total dust generation rate vs. material mass flow, each with one standard deviation confidence limit.

FIGURE 4--Total dust generation rate vs. moisture content, each with one standard deviation confidence limit.

FIGURE 5--Entrained air normalized to material mass flow vs. drop height.

FIGURE 6--Entrained air normalized to material mass flow vs. material mass flow.

FIGURE 7--Measured size specific dust generation rate vs. predicted size specific generation rate from Eqs. 8-11.

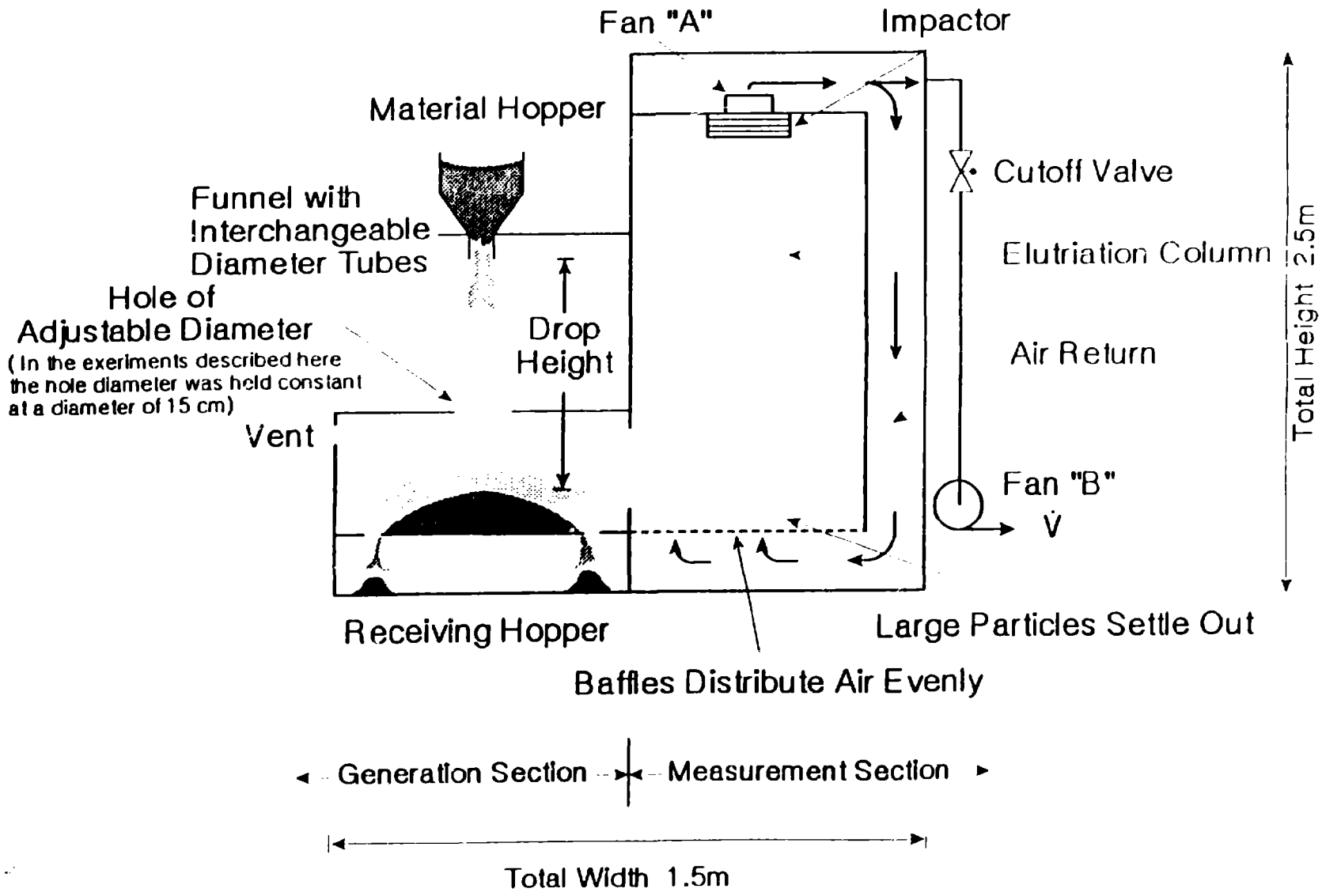
Fan "A"
Impactor
Material Hopper
Cutoff Valve
Funnel with
Interchangeable
Diameter Tubes
Elutriation Column
Hole of
Adjustable Diameter
(In the exeriments described here
the hole diameter was held constant
at a diameter of 15 cm)
Drop
Height
Air Return
Total Height 2.5m
Vent
Fan "B"
V̇
Receiving Hopper
Large Particles Settle Out
Baffles Distribute Air Evenly
Generation Section
Measurement Section
Total Width 1.5m

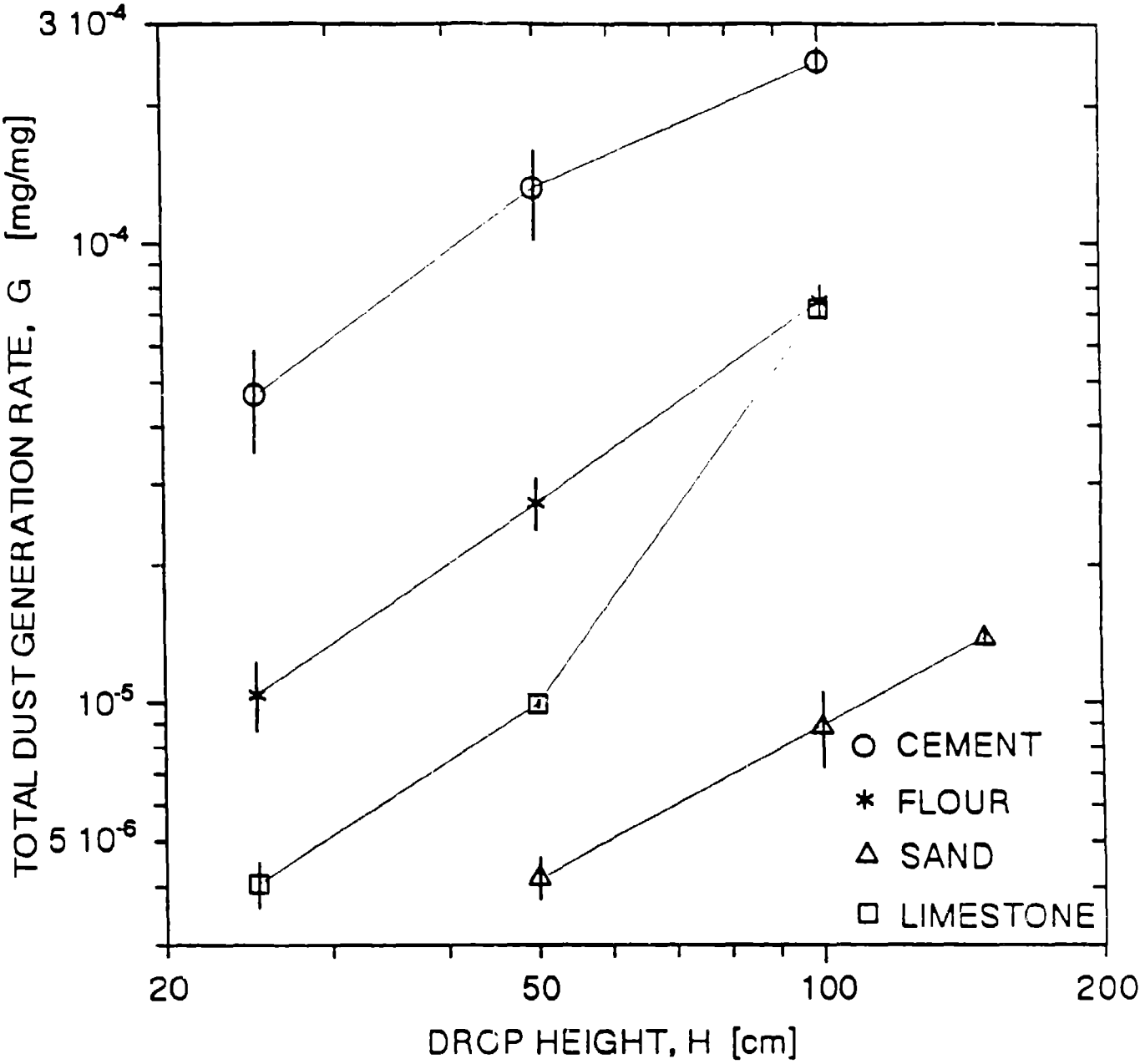
3 10-4
10-4
10-5
5 10-6
TOTAL DUST GENERATION RATE, G [mg/mg]
20
50
100
200
DROP HEIGHT, H [cm]
CEMENT
FLOUR
SAND
LIMESTONE

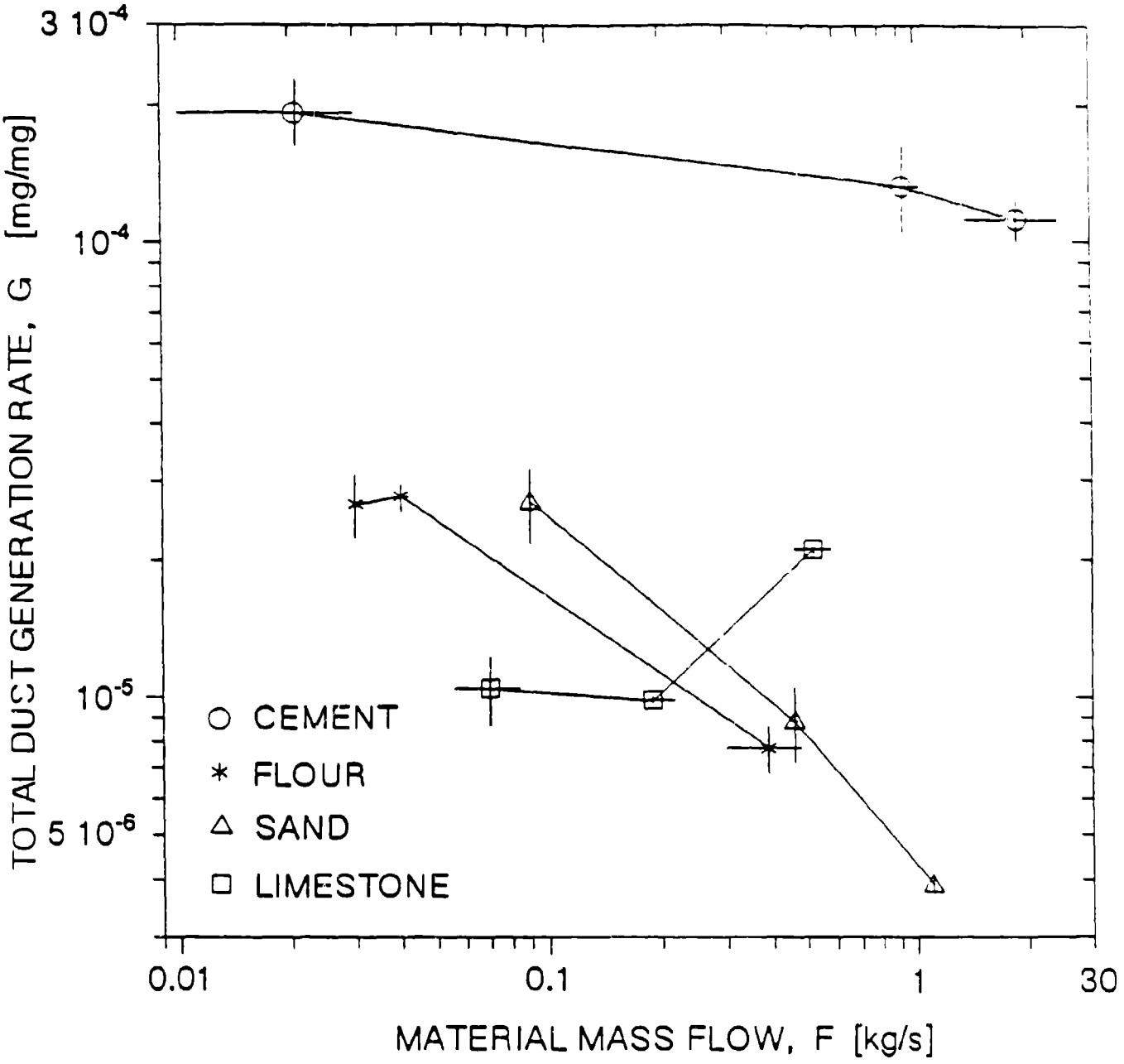
3 10-4
10-4
10-5
5 10-6
TOTAL DUST GENERATION RATE, G [mg/mg]
CEMENT
FLOUR
SAND
LIMESTONE
0.01
0.1
1
30
MATERIAL MASS FLOW, F [kg/s]

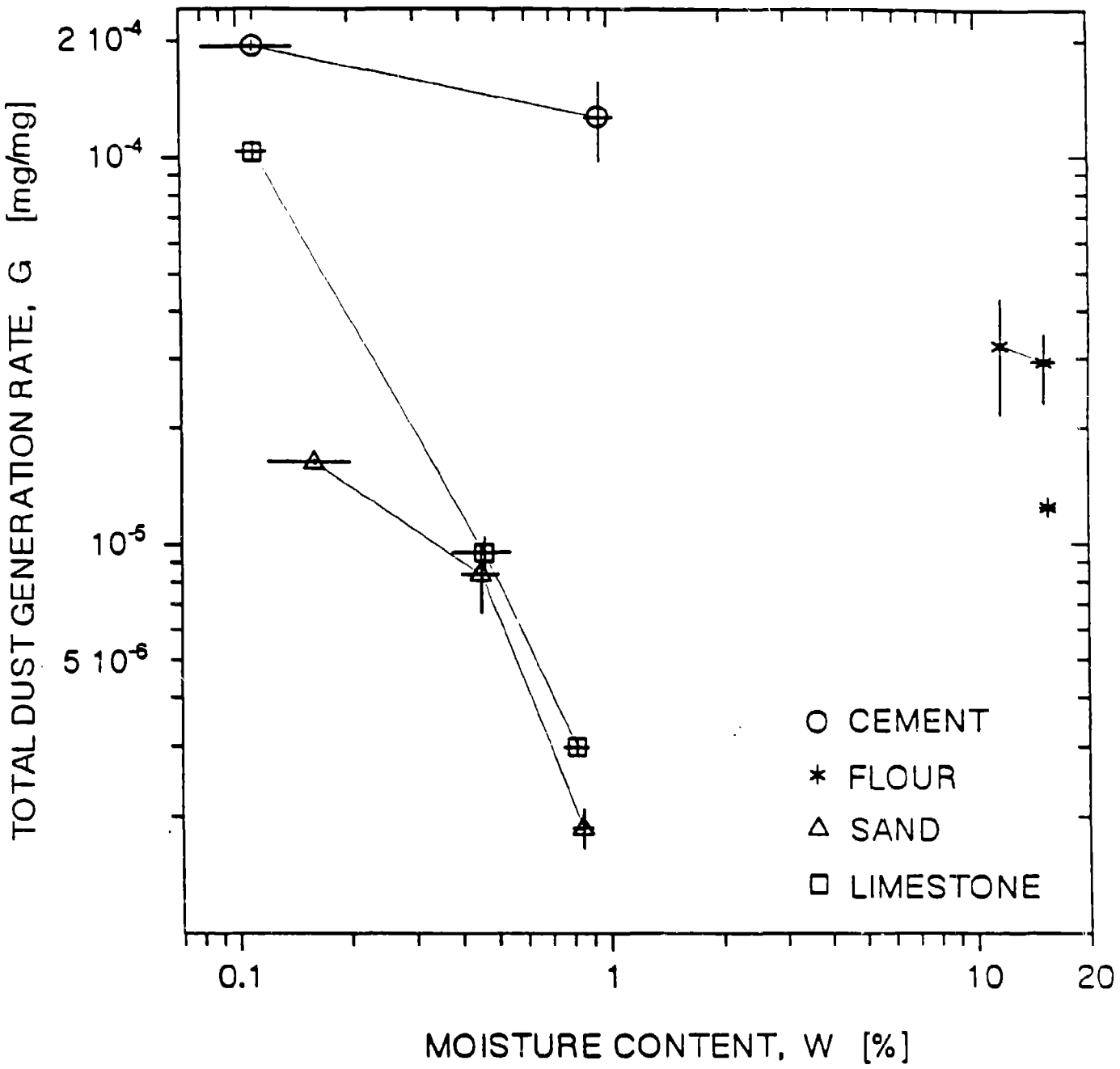
2 10⁻⁴
10⁻⁴
10⁻⁵
5 10⁻⁶
TOTAL DUST GENERATION RATE, G [mg/mg]
0.1
1
10
20
MOISTURE CONTENT, W [%]
CEMENT
FLOUR
SAND
LIMESTONE

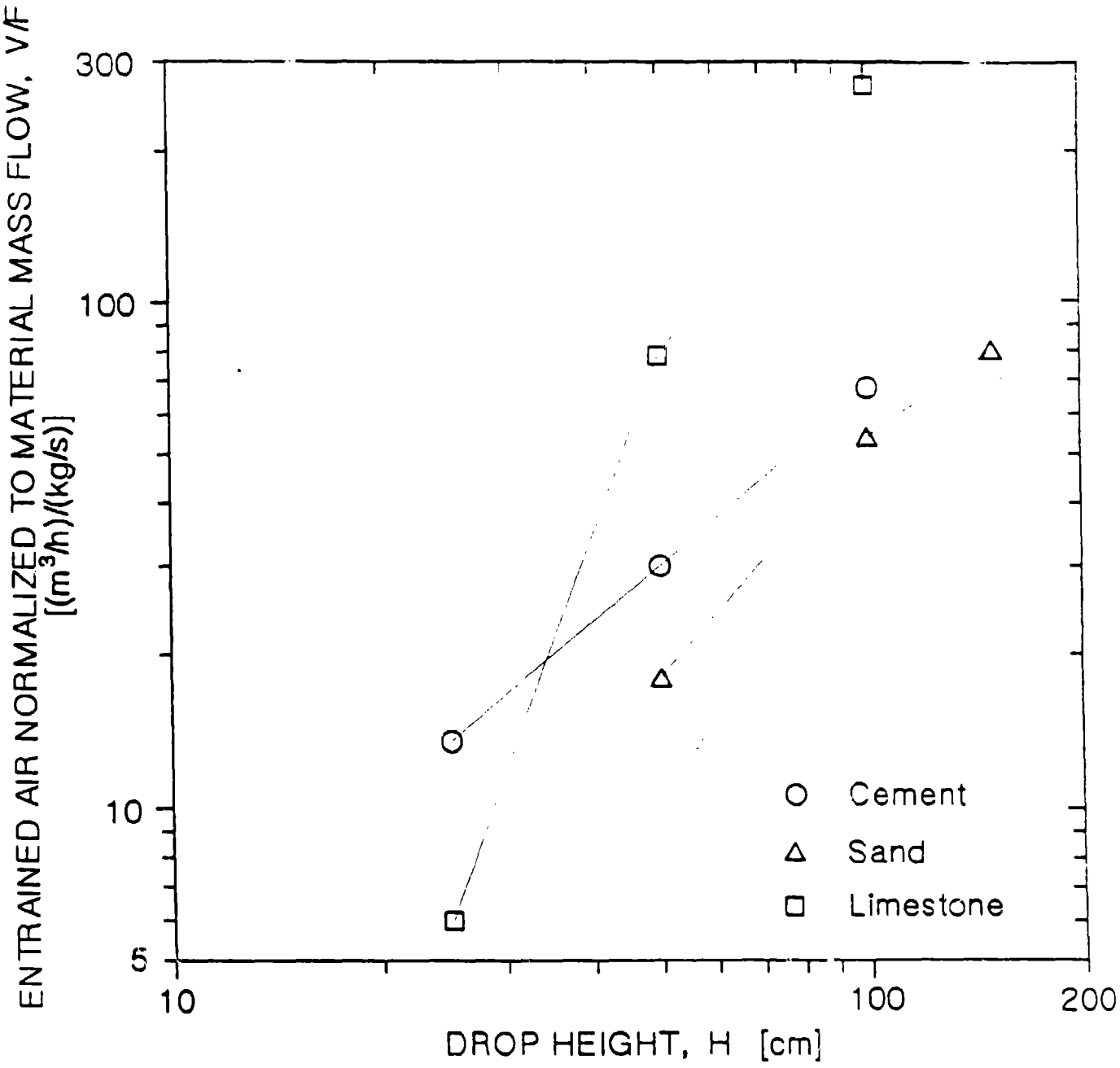
ENTRAINED AIR NORMALIZED TO MATERIAL MASS FLOW, $\dot{V}/\dot{F}$
[(m³/h)/(kg/s)]
300
100
10
5
10
100
200
DROP HEIGHT, H [cm]
Cement
Sand
Limestone

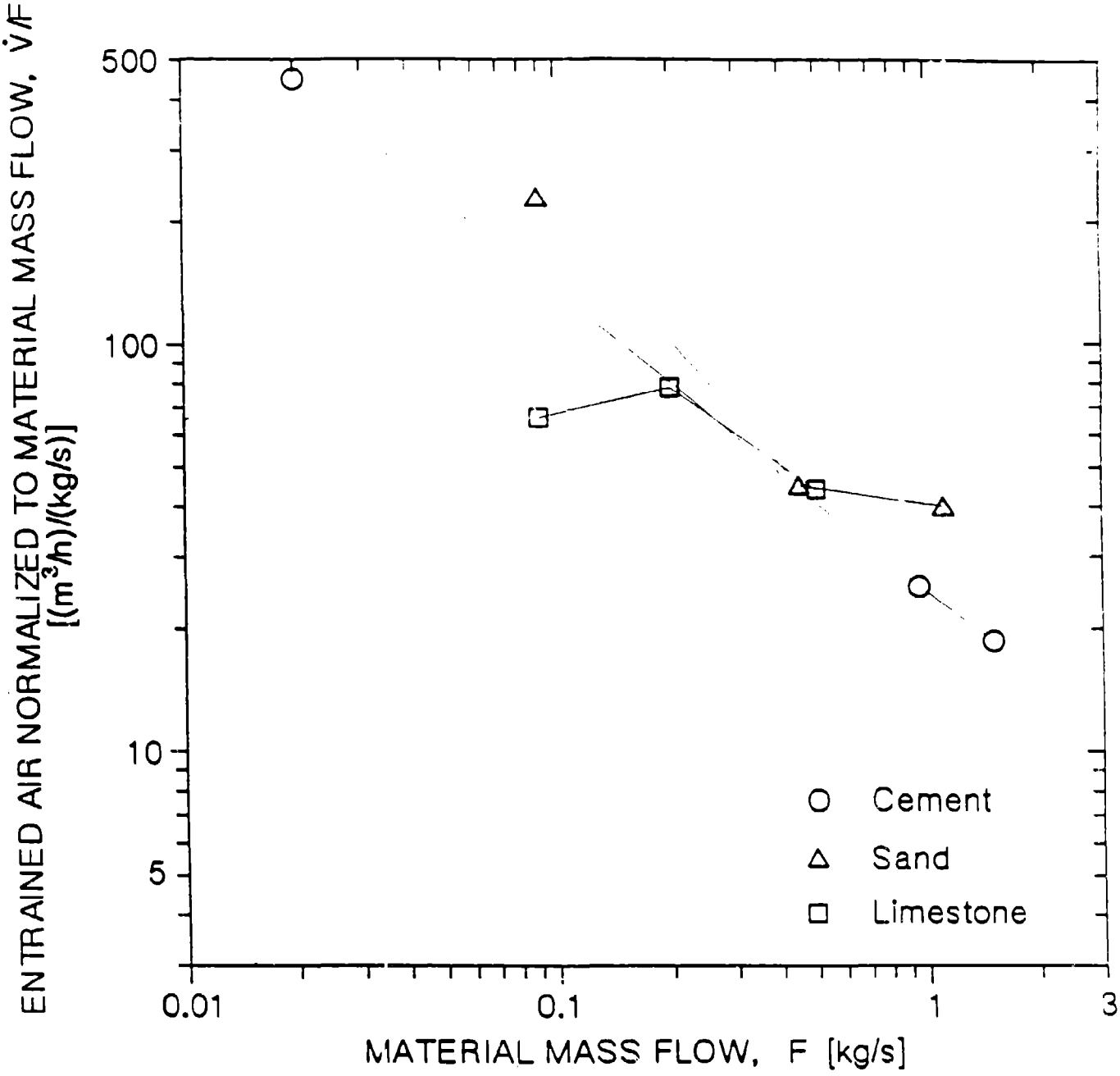
ENTRAINED AIR NORMALIZED TO MATERIAL MASS FLOW, V̇/F
[(m³/h)/(kg/s)]
500
100
10
5
0.01
0.1
1
3
MATERIAL MASS FLOW, F [kg/s]
Cement
Sand
Limestone

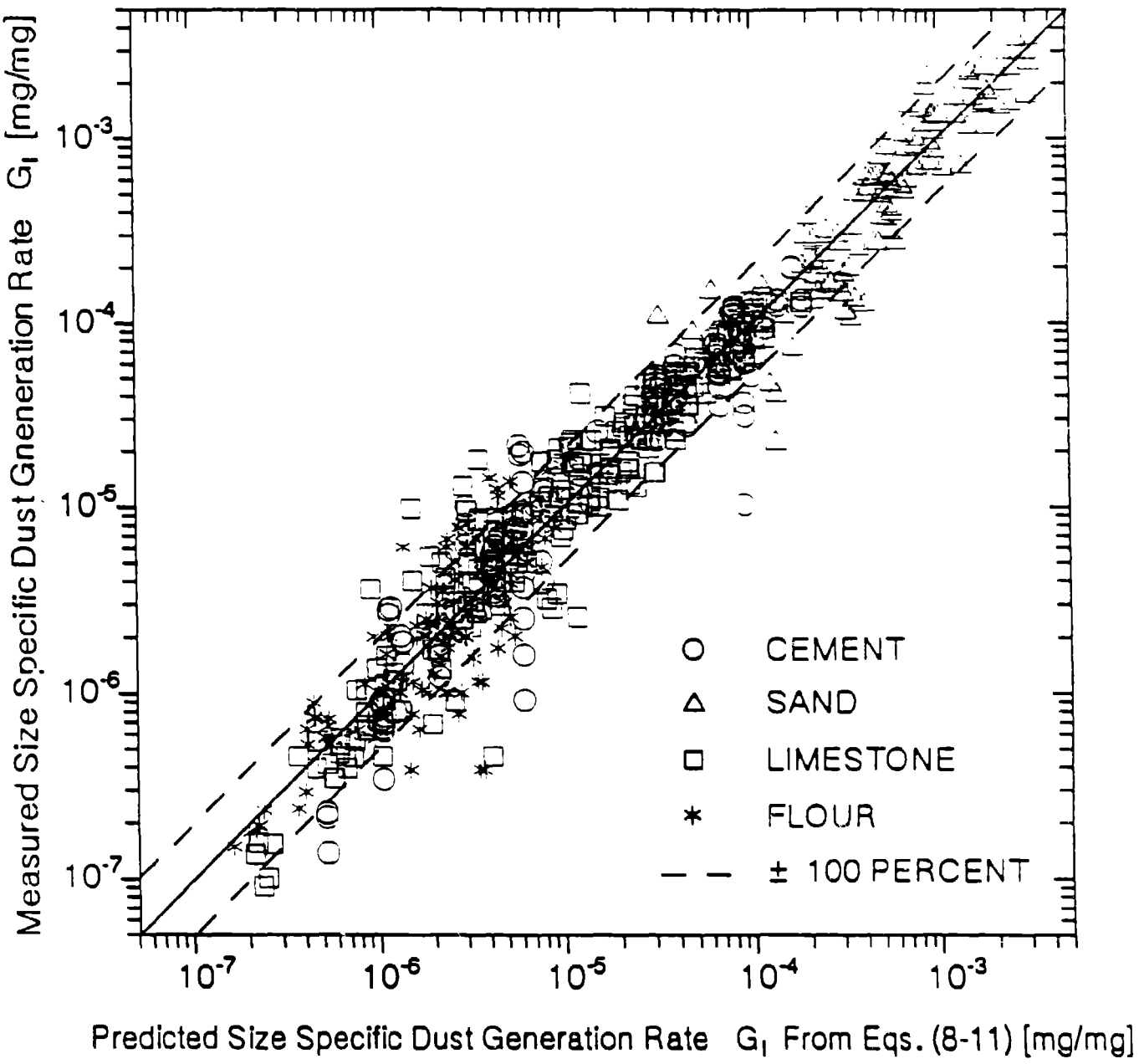
Measured Size Specific Dust Gneneration Rate G_I [mg/mg]
10^{-3}
10^{-4}
10^{-5}
10^{-6}
10^{-7}
10^{-7}
10^{-6}
10^{-5}
10^{-4}
10^{-3}
CEMENT
SAND
LIMESTONE
FLOUR
± 100 PERCENT
Predicted Size Specific Dust Generation Rate G_I From Eqs. (8-11) [mg/mg]

Experimental Examination of Factors that Affect Dust Generation using the Heubach and MRI Testers

MARC A.E. PLINKE, RALF MAUS, DAVID LEITH

Department of Environmental Sciences and Engineering, University of North Carolina at Chapel Hill, Chapel Hill, NC 27599

Abstract

Four factors that affect dust generation were investigated: test material, size distribution of the test material, moisture content of the test material, and apparatus used for the tests. Dust generated from silicon carbide and aluminum oxide was measured using MRI and Heubach dustiness testers modified to allow the measurement of dust size distribution using an Andersen impactor. The two materials investigated generated similar dusts. The size distribution of the test material slightly influenced the amount but strongly influenced the size distribution of the dust generated. Increased moisture content decreased the amount of dust generated but had little influence on dust size distribution. The two testers generated different amounts of dust, but the dust size distributions were similar. These results help explain factors that affect dust generation, and the relative importance of alternative methods for dust control.

BACKGROUND

Powders and granulated solids are used throughout industry. Handling these materials at transfer points, bagging, or dumping stations generates dust that may affect worker health or create a safety problem. To evaluate these hazards, the dust concentration in the breathing zone of the worker must be determined. Dust concentration depends on generation rate and dispersion. This research investigates factors that affect dust generation rate as a function of particle size.

Research in this field has been conducted with different goals in mind. The British Occupational Hygiene Society[1] established a working group in 1981 to establish a dustiness index scale for various materials. No standard procedure was found. Higman et al.[2] and Schofield[3] ranked the dustiness of nine materials using three dustiness devices. They found that moisture content and size distribution of the test material had a strong influence on dust generation. Cowherd and co-workers[4,5] at the Midwest Research Institute (MRI) developed a bench-top dust chamber to investigate the dust generation behavior of fourteen materials. They developed a model with four parameters to predict dust generation: moisture content, bulk density, mass median diameter, and geometric standard deviation of the size distribution for the test material. Other studies examined the problems of only one material or operation in industry. Hseih[6] showed the importance of moisture and size distribution changes to minimize losses of material in the alumina industry. Authier-Martin[7] investigated the influence of particle shape on dust generation. Despite this research, it is not possible to predict the size distribution or generation rate for dust produced in industry.

Heitbrink et al.[8-10] conducted a field study that attempted to correlate indices from the MRI and Heubach dustiness testers with dust exposures measured at two bag dumping and two bag filling operations. One dumping and one filling operation showed a relationship between dustiness test results and actual dust exposures, but two other operations showed no correlation. Because plant conditions, process variables, work habits, and body stature of the

worker affect breathing zone concentration but could not be investigated by a bench-top device to measure dustiness, Heitbrink et al. concluded that the relevance of dustiness tests to occupational dust exposures needs to be evaluated at each site.

Our work attempts to develop a more fundamental understanding of factors that affect dust generation. The overall objective of this research is similar to that of Heitbrink and others[1-5,8-10], to estimate the generation of respirable dust particles in industry. Figure 1 shows the approach taken here. Dust is generated when energy introduced to a granular material creates separation forces that drive particles of the material apart. An example of separation forces is the impact or inertia force developed when granules hit a surface. To generate dust, these separation forces must overcome interparticle binding forces; v.d. Waals, capillary, electrostatic forces and others. With knowledge of transport mechanisms from the dust generation site to the breathing zone of the worker, dust concentrations can be estimated.

Our working hypothesis asserts that the amount of dust generated is proportional to the fraction of particles with size "i" in the test material and depends on the ratio of the forces that separate particles to the forces that bind the particles,

$$\textit{Dust Generation Rate for Particles of Size "i"} = \textit{Fraction of Particles with Size "i" in Test Material} \quad f(\textit{Separation Forces/Binding Forces}) . \qquad (1)$$

This hypothesis rests on the assumption that the separation forces are insufficient to fracture particles; that is, all particles in the generated dust were present in the original material.

This work examines factors that affect dust generation: separation forces, binding forces, and the size distribution of the test material. The MRI and the Heubach dustiness testers treat material differently and so create different separation forces. Materials with different properties and moisture contents were tested to investigate the influence of binding forces on

dust generation. Samples of each material were prepared with different size distributions to determine the effect of material size on dust generation.

EXPERIMENTS

Apparatus

MRI Tester[4,8-10]

The MRI tester is shown in Figure 2. 270 cm^3 of material drops 25 cm onto a foam pad covered with aluminum foil. The generated dust is transported by 10 Lpm of air that enters the tester through two side baffles and leaves at the top. The dusty air was diluted with 18.3 Lpm of filtered room air before passing through a five stage Andersen ambient impactor with cut sizes from 1.1 to 7 μm.

Heubach Tester[8-10]

Figure 3 shows the Heubach apparatus. The dust generating pot is loaded with 20 grams of material, then rotates for two minutes at 30 RPM. Material within the pot periodically drops 6 cm from three inside-mounted paddles. The dust generated in two minutes is transported by a cross-air stream of 1.0 Lpm from the pot into the coarse dust separator. After dilution, the air stream passes through the same Andersen impactor used with the MRI tester.

Procedure

Test material

Silicon carbide and aluminum oxide (Micro Abrasives Cooperation, Westfield, MA) were chosen as two materials with different chemical but similar physical properties. An SEM examination showed that these materials consist of particles with no internal porosity. Neither reacts with water. To prevent agglomeration of the test material after moistening, the materials were sieved before each experiment.

Moisture content, W

The moisture content of the materials was determined by loss of weight per unit mass after drying. The moisture content of the material as received was its base value. Moisture content was raised by adding a measured amount of water to a known mass of material. Low moisture values were obtained by drying the material in a convection oven for five days at 140 °C.

The actual moisture content of the material was determined by averaging moisture measurements before and after the dustiness test to account for moisture reabsorbed from the environment. The moisture content of the test material in the Heubach tester was controlled by adjusting the moisture content of the air stream that transported dust through the dust pot. For experiments with dry material, the air stream was dried by passing it through a bed of Drierite. For experiments with moist material, the air stream was moistened by passing it through a bubbler.

Size distribution

"Fine", "middle-sized", and "coarse" samples of each material as defined by their mean diameter were obtained from the manufacturer. Their volumetric mean diameters as determined by Coulter Counter[11] analysis is in Table I. The three "pure" materials were mixed in different ratios to form ten additional blends as shown in Table II. For example, blend #13 was a mixture of 1 part fine material and 9 parts coarse material.

Measurements

The size specific dust generation rate, G_i, is defined as the fraction of dust particles generated with diameter "i".

$$G_i = (M_D)_i/(M_M)_i = (M_D)_i/(M_M{}^*Frac_i) \quad , \tag{2}$$

where:

$(M_D)_i$	mass of dust generated with size "i"
$(M_M)_i$	mass of test material with size "i"
M_M	total mass of test material, and

$Frac_i$ mass fraction of test material with size "i".

For example, a G_4 of 0.01 indicates that 1% of the 4 μm particles in the test material is generated and collected as a dust particle.

The total dust generation rate G is the ratio of the *total* mass of dust collected with the impactor to the *total* mass of material tested. G describes the dustiness of a material without consideration of either the size distribution of the original material or the size distribution of the dust generated.

$$G = M_D/M_M = \Sigma(M_D)_i \,/\, \Sigma(M_M)_i = \Sigma(M_D)_i \,/\, M_M \quad , \tag{3}$$

where:

M_D total mass of dust generated.

For example, a G of 0.01 indicates that 1% of the total mass of material becomes dust.

The cumulative size distribution of the generated dust[11] is represented by $Q_3(d)$.

$$Q_3(d) = \left[\sum_{d_{min}}^{d} (M_D)_i \right] / M_D \tag{4}$$

where:

d particle diameter

d_{min} minimum particle diameter of test material

This variable indicates whether the dust of one experiment is coarser or finer than the dust of another experiment, regardless of the size distribution of the materials tested. For example, $Q_3(4\ \mu m) = 0.7$ indicates that 70% of the dust is smaller than 4 μm in diameter.

Experimental Conditions

The number of experiments conducted was:

2 Apparatuses * 2 Materials * (13 Size Blends) * 3 Moistures = 156 Experiments.

Experiments were conducted in random order. The impactor stages were coated with silicone

oil to prevent particle bounce. A blank collection plate was weighed in all experiments. Calibration measurements were conducted once every fifteen experiments. During these calibration measurements, no material was dropped, and any weight changes on the impactor plates were recorded after the usual running time.

RESULTS

Statistical Analysis

An analysis of variance was conducted to determine the dependence of the dust generation rates G_i and G, and the dust size distribution $Q_3(d)$, on the dustiness tester, S, test material, T, moisture content, M, and the mass median diameter of the test material, d_{50}. The models for G_i and $Q_3(d)$ also included the cut size for each impactor stage d_i, and the fraction of particles with size "i" in the test material, $Frac_i$.

$$G,\ G_i,\ or\ Q_3(d) = const\ (S)^a(T)^b(M)^c(d_i)^e(d_{50})^f(Frac_i)^g\ , \qquad (5)$$

where

const	is a constant,
$S=1$	for MRI and $S=2$ for Heubach,
$T=1$	for aluminum oxide and $T=2$ for silicon carbide, and
a,b,c,e,f,g	are the calculated coefficients.

Coefficients determined for Eq. (5) are in Table III. No interaction terms were significant.

Graphical Examples of Important Dependencies

Figure 4 is a plot of the total dust generation rate, G, vs. material moisture content, M, for aluminum oxide as determined using the MRI tester. Lines are shown for four sizes of material: fine only, middle-size only, coarse only, and a 1:1:1 blend of fine, middle-size, and coarse materials. As expected, increasing moisture content reduces dust generation for all material sizes. From Table III, G is proportional to $M^{-0.3}$. For the same moisture content, finer material produces more dust. Table III shows that G is proportional to $d_{50}^{-0.4}$. The

blend of fine, middle, and coarse materials generates almost as much dust as the fine material alone. The lines for all materials have negative slopes and are almost parallel, which indicates that all size blends of the same material react similarly to added moisture. The largest point on each curve indicates the equilibrium moisture content of that specific blend in the lab environment. The smaller the particles are, the higher the equilibrium moisture content is.

Figure 5 shows the cumulative size distribution of the dust generated from fine aluminum oxide material for data taken with the Heubach tester. Lines are plotted for four moisture contents that range from 0.03% to 0.15%. The four size distributions are virtually identical, indicating that material moisture content had little effect on the size distribution of the dust generated. This trend is also shown in Table III, where M has no significant effect on $Q_3(d)$.

Figure 6 is a plot of the size specific dust generation rate G_i against dust particle diameter for fine aluminum oxide data taken using the Heubach tester. Data are shown for moisture contents that range from 0.03% through 0.15%. This figure shows that increasing moisture content decreases the amount of dust generated for all particle sizes. All lines have a positive slope; thus, the size specific dust generation rate increases with particle diameter. Table III confirms this trend as G_i was found to increase with $d_i^{2.2}$.

Figure 7 shows a series of cumulative size distributions. The lines marked "A" and "B" are for the fine and middle-sized *material*. The other five lines in Figure 7 are for *dust* generated from testing blends of these two materials. The size distributions for the generated dust show that if more fine material is present, the size distribution of the generated dust becomes finer as well.

However, the size distribution of the dust generated does not match directly the size distribution of the original material. For example, dust generated from the fine material is not as fine as the parent material itself. Similarly, dust generated from the middle-sized material is generally not as fine as the parent material itself. Blends of up to 50% middle-sized

material with fine material produce dust particles that have size distributions similar to particles of dust from fine material alone.

DISCUSSION

Influence of the test method on dust generation

The Heubach tester generates about $2^{2.5} \approx 6$ times more dust than the MRI tester as seen in Table III column "*S*"; *the S* value for the Heubach Tester was 2; the coefficient for Eq. (5) was 2.5. In the Heubach tester, material drops 180 times from about 6 cm during the 2 minute duration of an experiment, whereas in the MRI tester the material drops only once from 25 cm. In short, the total energy input per mass of material in the Heubach tester is approximately 42 times higher than the energy input per mass of material in the MRI tester. Earlier research[13-15] has shown that the amount of dust generated increases proportionally with potential energy. Thus, the Heubach tester did not generate as much dust as expected. This behavior cannot yet be explained.

For the same testing conditions, the Heubach and the MRI testers produced dust with essentially the same size distributions. Table III shows that the particle size distribution of the generated dust was not affected by the dust generation method as Q_3 is independent of variable *S*.

Influence of the test material

Both aluminum oxide and silicon carbide generated the same amount of dust with the same size distribution when treated in the same way; that is, no difference in dust generation from material to material was found. Table III shows that neither G_i nor Q_3 was dependent on test material *T*. This finding suggests that the influence of chemical properties that depend on the makeup of the material were less significant for dust generation in these tests than the influence of physical properties such as moisture content or material size distribution.

Influence of material moisture content

In Figure 5, the cumulative size distributions for the same material with different moisture contents overlap. Thus, moisture content did not affect the size distribution of the dust generated. This trend can also be seen in Figure 6, where increasing the moisture content of the test material decreased dust generation rate uniformly for both small and large particles.

For the two crystalline, nonreactive, and nonporous materials used here, added moisture should build a liquid layer on particle surfaces. Increasing this layer should increase the capillary forces that bind particles together. The moisture content of the test material in equilibrium with lab air increased with decreasing particle size. This suggests the presence of sorption layers of water on the surface of particulate matter prior to artificial moistening. The extent of these layers depends on the specific surface of the material, which increases as particle size decreases.

Influence of the size distribution of the test material

The size specific dust generation rate G_i increased with increasing particle diameter (see Figure 6, where relatively more 6 μm particles were generated than smaller, 1 μm particles. Table III also shows that G_i increases with increasing particle size, d_i. A reason for this behavior is that a separation force such as impaction increases with d_i^3 whereas binding forces due to v.d. Waals attraction and capillary forces are proportional[14-17] to d_i. Thus, as particle size increases, separation forces increase more rapidly than binding forces.

Figure 4 shows that materials blended to contain only a portion of small particles are nearly as dusty as materials comprised entirely of small particles. This trend is also shown in Table III, where G_i increases as the fraction of particles with size "i" in the parent material, $Frac_i$, decreases. As the proportion of small particles in a blend diminishes, the fraction of these small particles generated as dust increases. Consequently, a partial extraction of the small, respirable particles of a material does not decrease the amount of dust generated in a

proportional way. Instead, the amount of dust generated may only decrease slightly. This trend is shown in Figure 7. Increasing the moisture content is more effective to reduce dustiness than to extract small particles.

Overlaying the role of separation and binding forces in dust generation is particle transport away from the dust generation site. For particles $< 10\ \mu m$, gravity does not substantially affect short-range transport. However, gravity does prevent transport of large particles from the dust generation site to the breathing zone of the worker or to the measuring site.

CONCLUSIONS

The dust generation rate of silicon carbide and aluminum oxide has been investigated by the Heubach and MRI dustiness testers. The influence of moisture content of the test material and material size distribution were studied by measuring the amount and size distribution of the dust generated.

The amount of dust generated by the two test devices differed by a factor of 6 but was not directly proportional to energy input. The size distribution of the dusts generated by the two test devices were similar. The use of only one dustiness tester for future research appears sufficient to investigate factors that affect dust generation and size distribution.

For the aluminum oxide and silicon carbide tested here, material chemical properties were not as important as physical properties such as moisture content and size distribution. The two chemically different but physically similar materials generated similar dust.

Increases in moisture content decreased the amount of dust generated for all particle sizes.

Extracting small particles from a material did not decrease proportionally the amount of dust generated. Therefore, where possible, dust suppression is best accomplished by adding moisture to the test material.

ACKNOWLEDGEMENT

This project was supported by grant 1R01 OH02437-01 from the National Institute for Occupational Safety and Health of the Centers for Disease Control and by EPA Cooperative Agreement CR-818060-01-0. The authors wish to thank Friedrich Löffler, Karlsruhe Germany and Maryanne G. Boundy of the University of North Carolina for their support and advice.

REFERENCES

1. **British Occupational Hygiene Society Technology Committee Working Party on Dustiness Estimation:** Progress in dustiness estimation. *Ann. Occup. Hyg.* 32(4):535-544 (1988).

2. **Higman, R.W., C. Schofield, and M. Taylor:** "Bulk material dustiness, an important material property - its measurement and control." 4th International Environment and Safety Conference, Barbicon Center, London, Mar. 27-9, 1984.

3. **Schofield, C.:** Dust generation and control in materials handling. *Bulk Solids Handling* 1(3):419-427 (1981).

4. **Cowherd Jr., C., M. A. Grelinger, P. J. Englehart, R. F. Kent, and K. F. Wong:** An apparatus and methodology for predicting the dustiness of materials. *Am. Ind. Hyg. Assoc. J.* 50(3): 123-130 (1989).

5. **Cowherd Jr., C., M. A. Grelinger, and K. F. Wong:** Dust inhalation exposures from the handling of small volumes of powders. *Am. Ind. Hyg. Assoc. J.* 50(3):131-138 (1989).

6. **Hsieh, H. P.:** "Measurement of flowability and dustiness of alumina." Light Metals. 1987: Proceedings of Sessions, Ammerican Institute of Mining, Metallurgical, and Petroleum Engineers (AIME) Annual Meeting, Metallurgical Soc. of AIME, Warrendale, PA. p.139-49, 1987.

7. **Authier-Martin, M.:** "Alumina handling dustiness." Light Metals, 1989: Proceedings of Sessions, AIME Annual Meeting, Metallurgical Soc. of AIME, Warrendale, PA. p.103-11, 1989.

8. **National Institute for Occupational Safety and Health:** *Evaluation of Dustiness Test Methods and Recommendations for Improved Dust Control at Heubach Inc. Newark, New Jersey* by T.C.Cooper, W.A.Heitbrink and D.M.O'Brien (NIOSH Report No. ECTB 154-11a). Cincinatti, Ohio, February 1989.

9. **Heitbrink, W. A., W. F. Todd, T. C. Cooper, D. M. O'Brien:** The Application of Dustiness Tests to the Prediction of Worker Dust Exposure. *Am. Ind. Hyg. Assoc. J.* 51(4):217-223 (1990).

10. **National Institute for Occupational Safety and Health:** *Exposure estimation procedure for powder handling operation based on dustiness testing* by W.A.Heitbrink and D.M.O'Brien. Engineering Control Technology Branch, Division of Physical Sciences and Engineering, Cincinatti Ohio, 1989.

11. **Rumpf, H.:** *Particle Technology*, 1st ed. New York: Chapman And Hall, 1990.

12. **Systat Inc:** *Systat the System for Statistics*, 603 Main St., Evanston, Il, 1985.

13. **R. Bohn, T. Cuscino Jr. and C. Cowherd Jr.:** *Fugitive emissions from integrated iron and steel plants*. EPA Report EPA-600/2-78-050), Office of Research and Development, Washington DC, 20460, March 1978.

14. **US Environmental Protection Agency:** *Compilation of Emission Factors*. 3rd ed., Supplement No. 14, NTIS, Office of Air Quality Planning and Standards, Springfield, VA. p.11.23-3, 1983.

15. **Plinke, M., D. Leith, D. B. Holstein, and M. G. Boundy:** Experimental Examination of Factors that Affect Dust Generation. Accepted for publication. *Am. Ind. Hyg. Assoc. J.* (1991).

16. **Krupp, H.:** *Advances in Colloid and Interface Science*. 1: 111 (1967).

17. **Rumpf, H.:** Die Wissenschaft des Agglomerierens. *Chemie-Ing.-Tech.* 46(1):1-11 (1974).

Table I

Volumetric mean diameter of silicon carbide and aluminum oxide

	fine	middle-sized	coarse
Silicon carbide	4 μm	7 μm	25 μm
Aluminum oxide	3 μm	6 μm	25 μm

Table II

Mixing proportions for silicon carbide and aluminum oxide

Blend #	1	2	3	4	5	6	7	8	9	10	11	12	13
fine	1	-	-	1	1	1	-	9	9	-	-	1	1
middle	-	1	-	1	1	-	1	1	-	9	1	9	-
coarse	-	-	1	1	-	1	1	-	1	1	9	-	9

Table III

Coefficients for Eq. (5)

	const	*S*	*T*	*M*	d_i	d_{50}	$Frac_i$	*R2*
G_i	80	2.5	-	-0.3	2.2	-	-0.6	84
G	5884	2.5	-	-0.3	n	-0.4	n	86
$Q_3(d)$	1	-	-	-	2.8	-	+0.3	89

FIGURE CAPTIONS

Figure 1--Model of dust generation processes

Figure 2--Schematic diagram of MRI tester.

Figure 3--Schematic diagram of Heubach Dust Measurement Appliance.

Figure 4--Total dust generation rate vs. moisture content.

Figure 5--Cumulative size distribution of the dust generated vs. aerodynamic particle diameter.

Figure 6--Specific dust generation rate vs. aerodynamic particle diameter.

Figure 7--Cumulative size distribution of the test material and dust generated vs aerodynamic particle diameter.

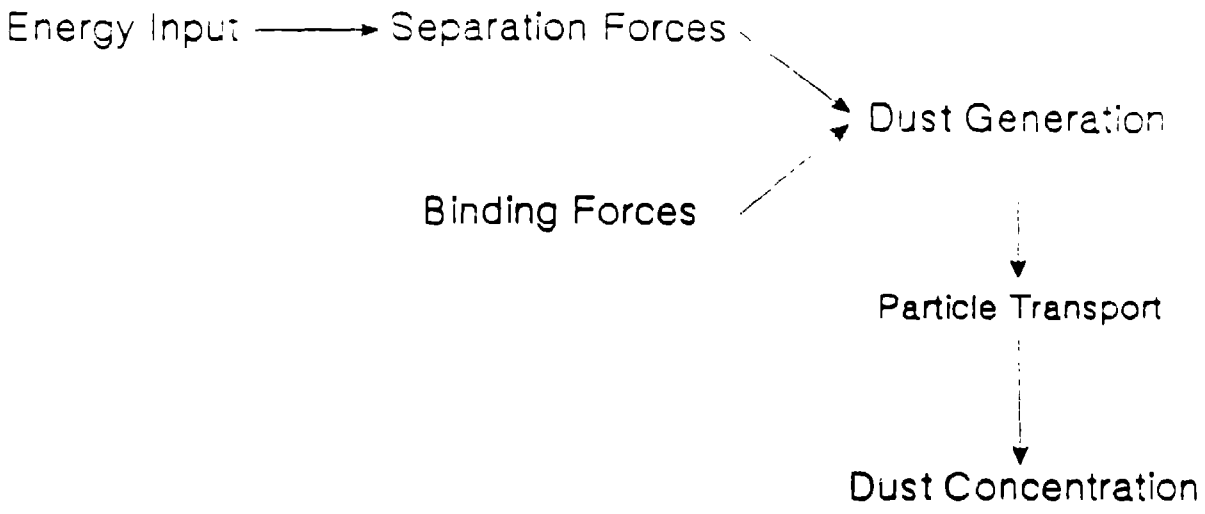
Energy Input
Separation Forces
Dust Generation
Binding Forces
Particle Transport
Dust Concentration

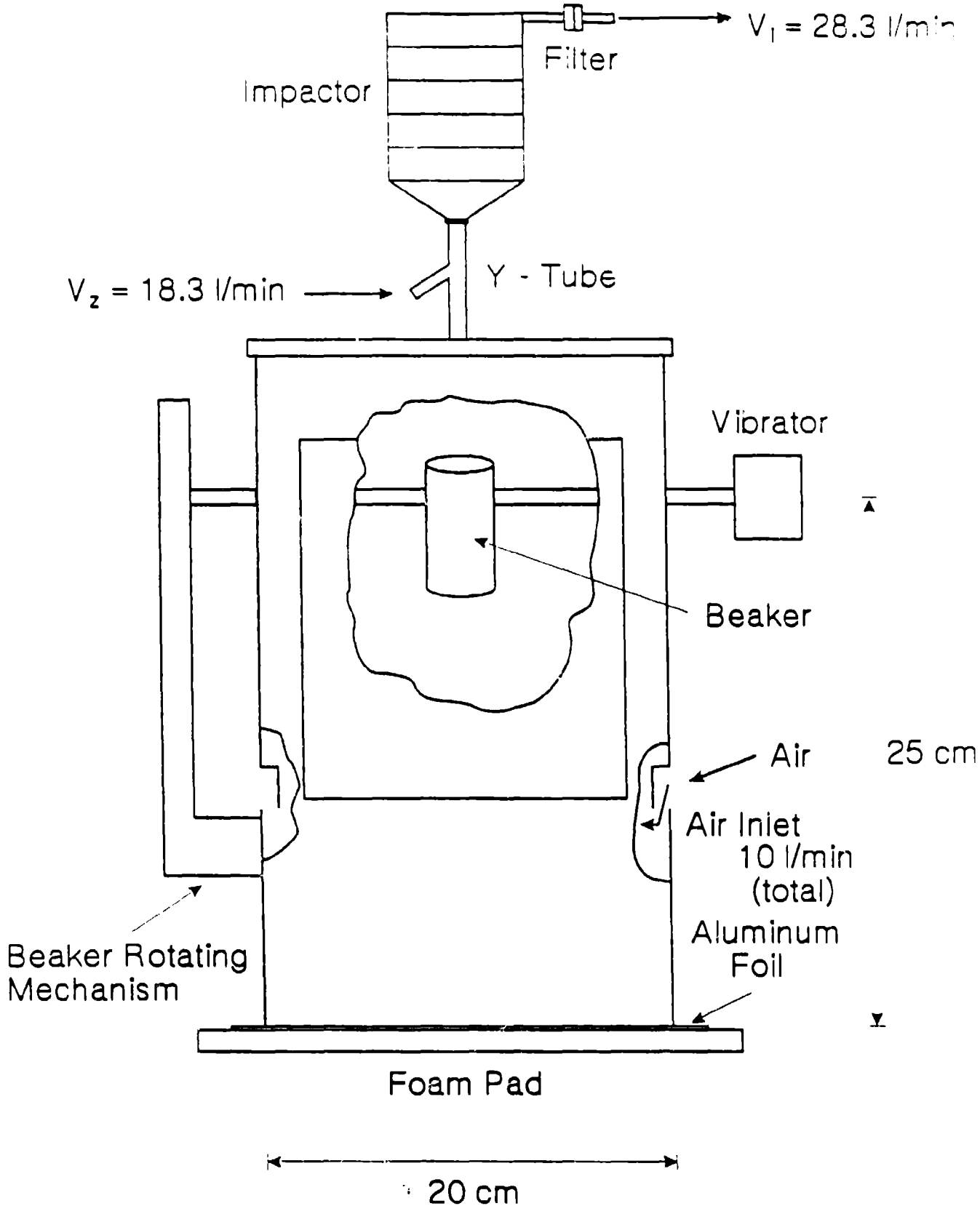
V_1 = 28.3 l/min
Filter
Impactor
V_2 = 18.3 l/min
Y - Tube
Vibrator
Beaker
Air
25 cm
Air Inlet
10 l/min
(total)
Aluminum
Foil
Beaker Rotating
Mechanism
Foam Pad
20 cm

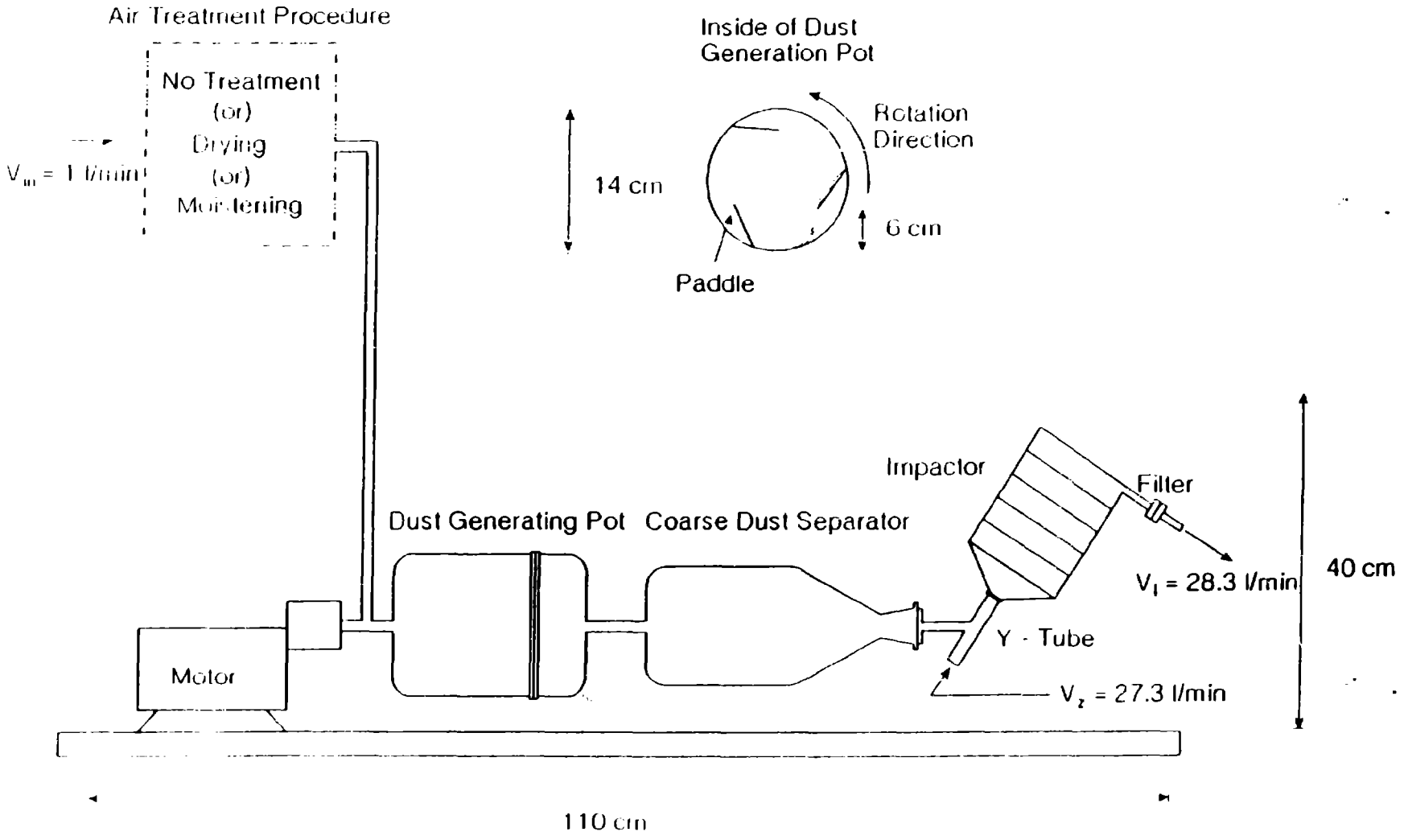
Air Treatment Procedure
No Treatment
(or)
Drying
(or)
Moistening
V_{in} = 1 l/min
Inside of Dust
Generation Pot
14 cm
Rotation
Direction
6 cm
Paddle
Impactor
Filter
Dust Generating Pot
Coarse Dust Separator
V_1 = 28.3 l/min
40 cm
Y - Tube
Motor
V_2 = 27.3 l/min
110 cm

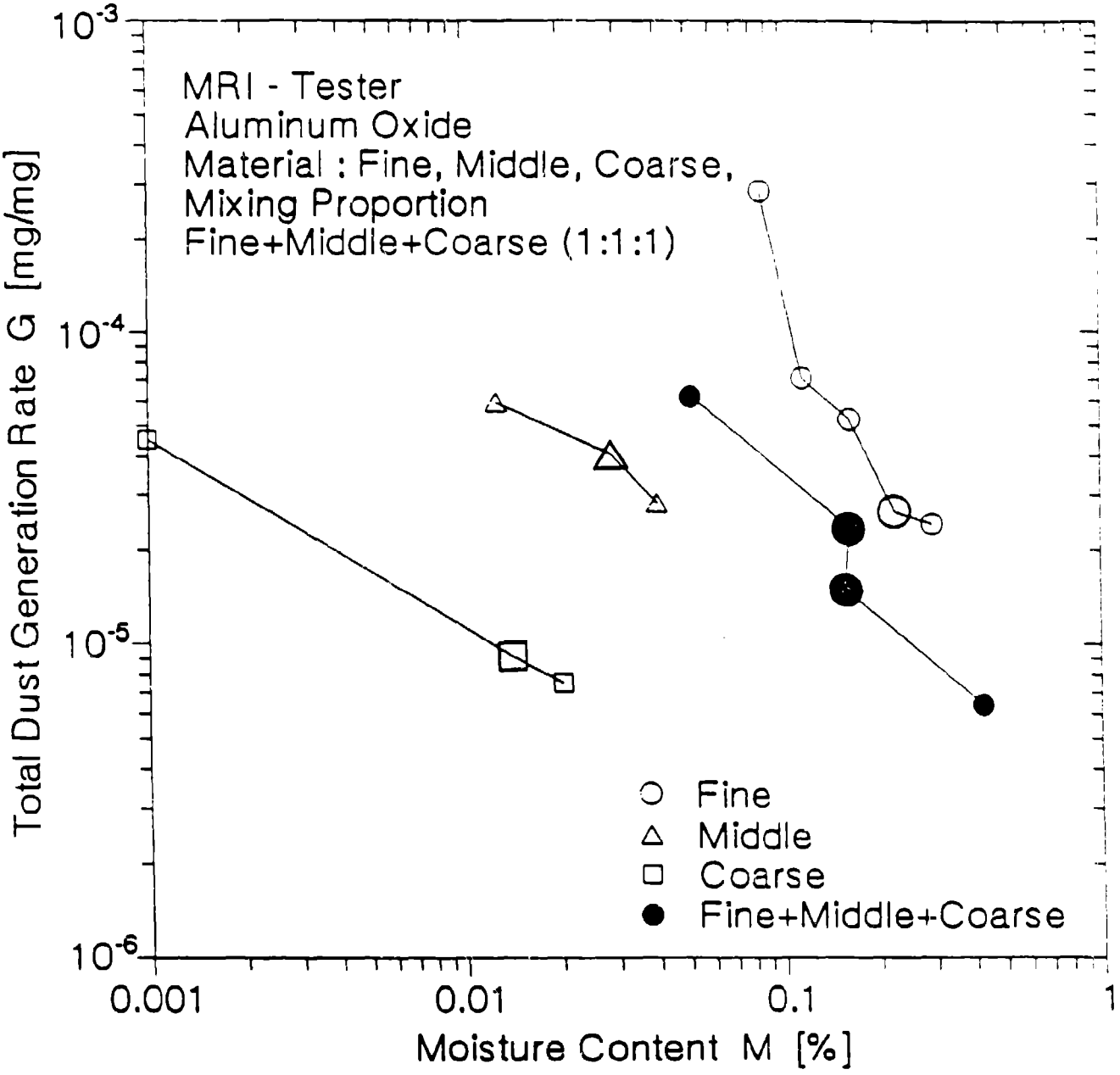
MRI - Tester
Aluminum Oxide
Material : Fine, Middle, Coarse,
Mixing Proportion
Fine+Middle+Coarse (1:1:1)
Total Dust Generation Rate G [mg/mg]
Moisture Content M [%]
10-3
10-4
10-5
10-6
0.001
0.01
0.1
1
Fine
Middle
Coarse
Fine+Middle+Coarse

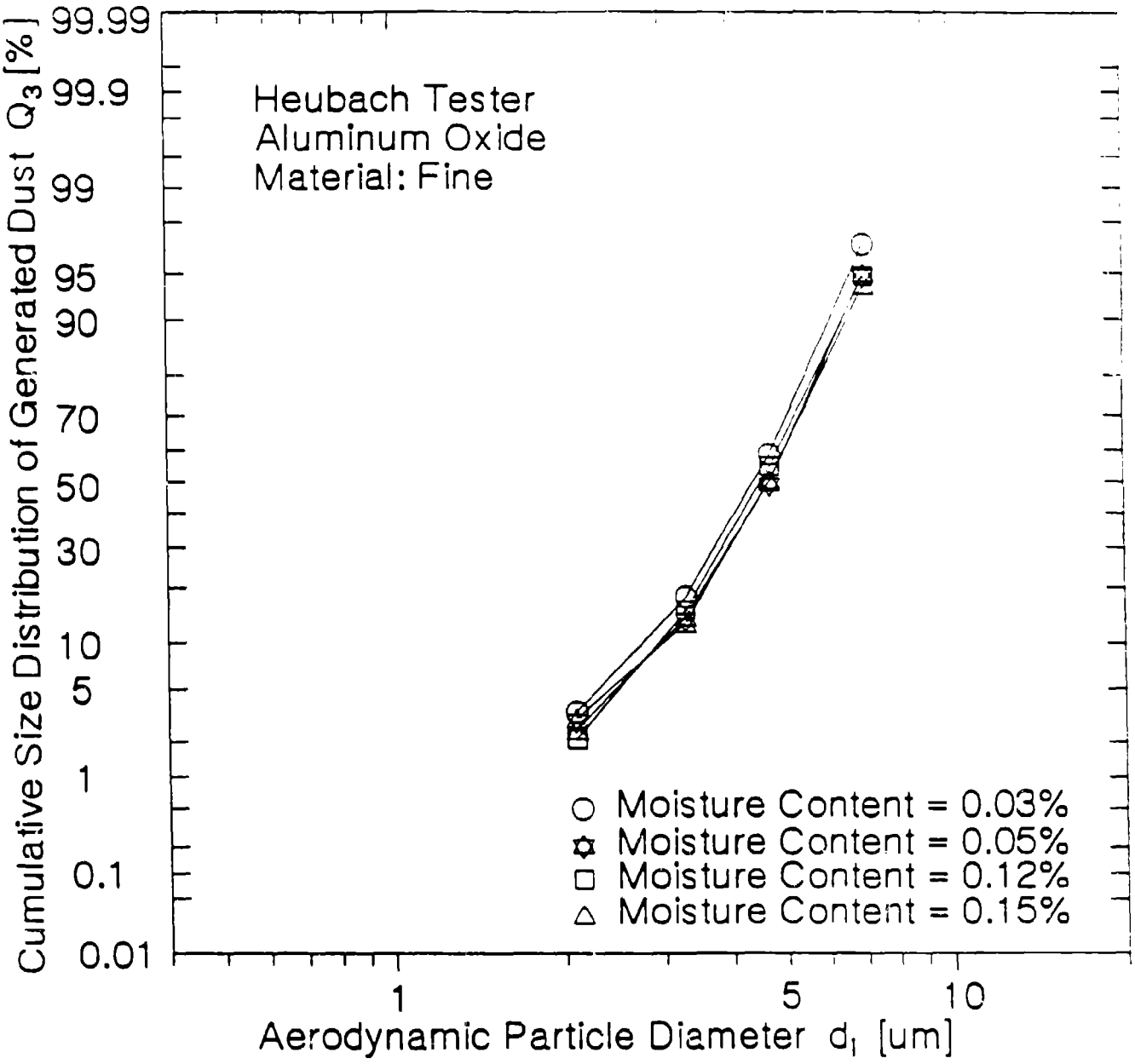
Heubach Tester
Aluminum Oxide
Material: Fine
Cumulative Size Distribution of Generated Dust Q_3 [%]
99.99
99.9
99
95
90
70
50
30
10
5
1
0.1
0.01
1
5
10
Aerodynamic Particle Diameter d_1 [um]
Moisture Content = 0.03%
Moisture Content = 0.05%
Moisture Content = 0.12%
Moisture Content = 0.15%

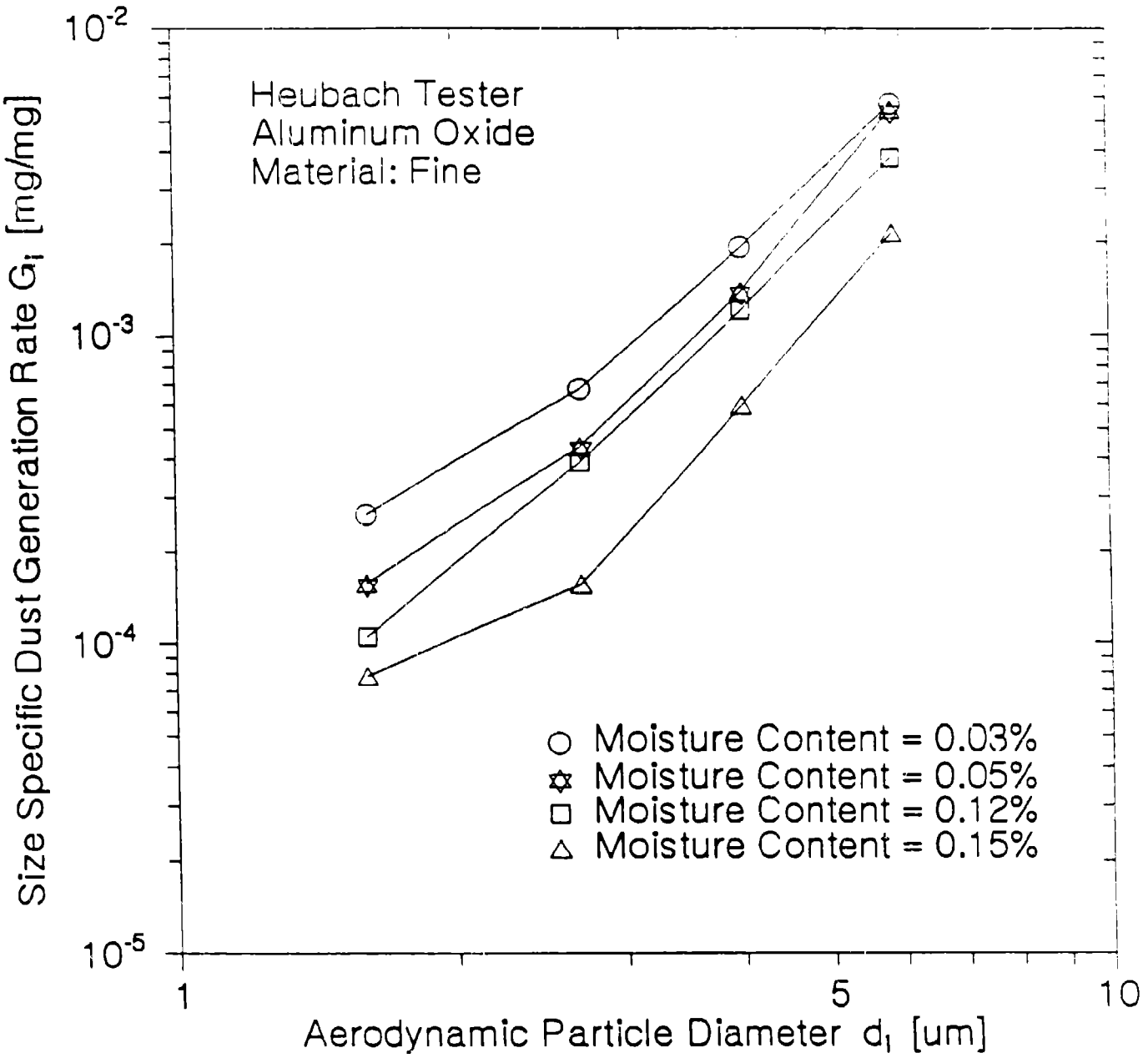
Heubach Tester
Aluminum Oxide
Material: Fine
Size Specific Dust Generation Rate G_i [mg/mg]
10^{-2}
10^{-3}
10^{-4}
10^{-5}
1
5
10
Aerodynamic Particle Diameter d_i [um]
Moisture Content = 0.03%
Moisture Content = 0.05%
Moisture Content = 0.12%
Moisture Content = 0.15%

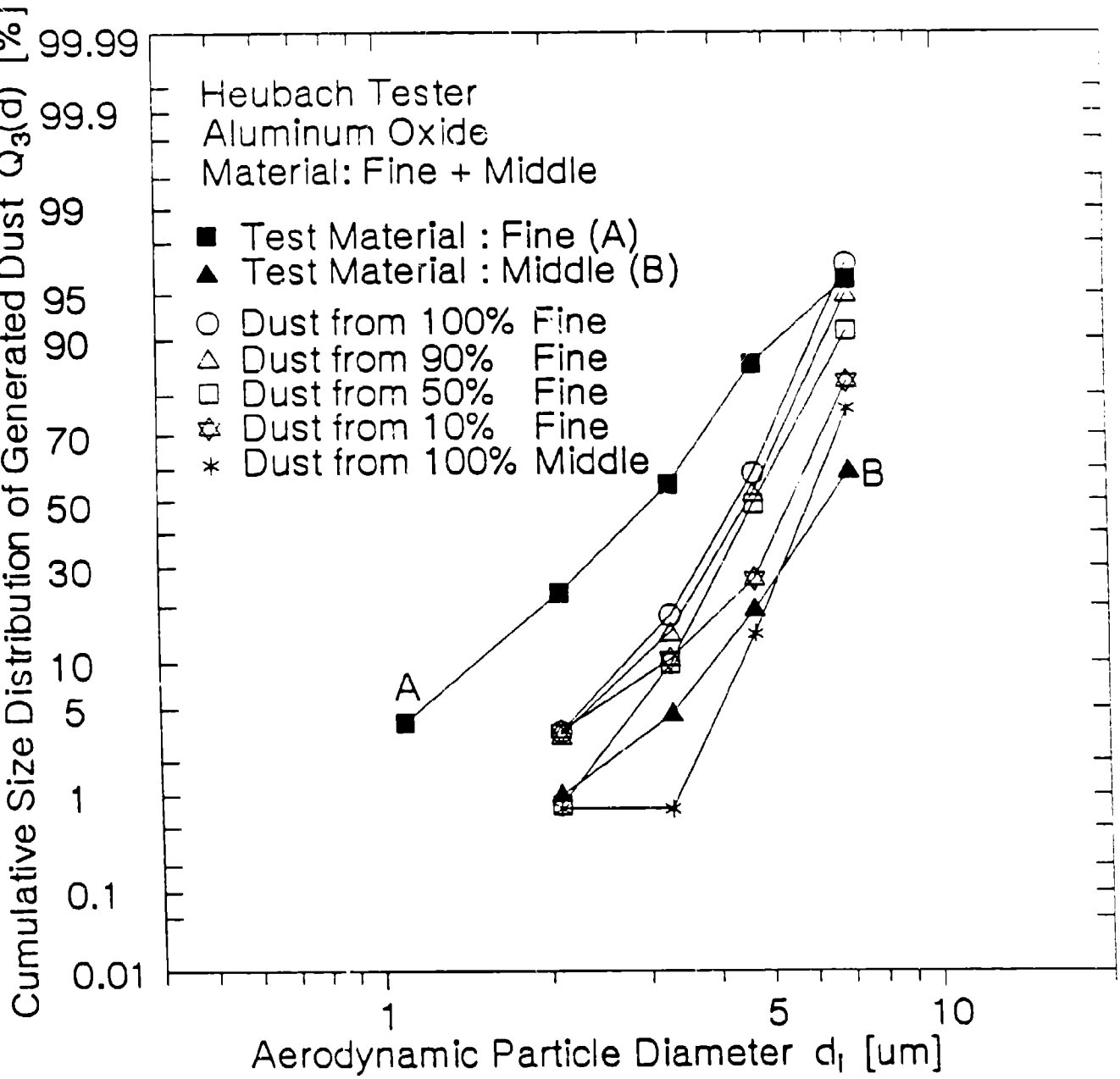
Heubach Tester
Aluminum Oxide
Material: Fine + Middle
Test Material : Fine (A)
Test Material : Middle (B)
Dust from 100% Fine
Dust from 90% Fine
Dust from 50% Fine
Dust from 10% Fine
Dust from 100% Middle
A
B
Cumulative Size Distribution of Generated Dust $Q_3(d)$ [%]
99.99
99.9
99
95
90
70
50
30
10
5
1
0.1
0.01
1
5
10
Aerodynamic Particle Diameter d_I [um]